USING (MICROCHANNEL) ELECTROCHEMICAL IMPEDANCE SPECTROSCOPY TO DETECT BACTERIAL ACTIVITIES

A Dissertation

presented to

the Faculty of the Graduate School

at the University of Missouri - Columbia

In Partial Fulfillment

of the Requirements for the Degree

Doctor of Philosophy

by

YONGQIANG YANG

Dr. Shramik Sengupta, Dissertation Supervisor

DECEMBER 2020

The undersigned, appointed by the dean of the Graduate School, have examined the Dissertation entitled

USING (MICROCHANNEL) ELECTROCHEMICAL IMPEDANCE SPECTROSCOPY TO DETECT BACTERIAL ACTIVITIES

Presented by Yongqiang Yang

A candidate for the degree of Doctor of Philosophy in Biological Engineering and hereby certify that, in their opinion, it is worthy of acceptance.

Dr. Shramik Sengupta, Department of Biological Engineering

Dr. Raghuraman Kannan, Department of Biological Engineering

Dr. Kevin Gillis, Department of Biological Engineering

Dr. Caixia Wan, Department of Biological Engineering

Dr. Azlin Mustapha, Department of Food Science

To my wife, my son, my daughter, my parents, and my parents-in-law

ACKNOWLEDGMENTS

I want to thank my academic advisor and committee chairman, Dr. Shramik Sengupta, for sharing his knowledge and experience. I was fortunate to work with him. He gave me the wonderful experience of working on these worthwhile projects, and his tireless endeavors toward academic accomplishment inspired me. He put great effort into training me. I would also like to thank my other committee members, Dr. Raghuraman Kannan, Dr. Kevin Gillis, Dr. Azlin Mustapha, and Dr. Caixia Wan for helping me to complete my Ph.D. studies. Also, I am very thankful to Dr. Swiger and Impedx Diagnostics Inc. for their supports.

Furthermore, I would like to thank my friends and colleagues, Dr. Roli Kargupta, Dr. Sachidevi Puttaswamy, and Amandeep Sharma, for providing me with great advice.

I would especially like to thank my father and my parents-in-law. In the past years, they came to the United States to help us with the daily responsibilities of housework and caring for my son and daughter. So, I could have more time to work on our projects and research.

Finally, I would like to thank my wife, son, daughter, parents, and brother for their love, support, and encouragement.

TABLE OF CONTENTS

page

LIST OF TABLES

Table page

LIST OF FIGURES

Figure page

LIST OF ABBREVIATIONS

EIS	Electrochemical Impedance Spectroscopy
m-EIS	microchannel Electrochemical Impedance Spectroscopy
TB	Tuberculosis
Mtb	*Mycobacterium Tuberculosis*
LAB	Lactic Acid Bacteria
TTD	Time to Detection

USING (MICROCHANNEL) ELECTROCHEMICAL IMPEDANCE SPECTROSCOPY TO DETECT BACTERIAL ACTIVITIES

By

Yongqiang Yang

Dr. Shramik Sengupta, Dissertation Supervisor

ABSTRACT

Even though rapid detection of molecular methods has been used in bacterial detection, (automated) liquid culture methods are still the “Gold Standard” for the detection of living bacteria, especially in cases where there may be similar dead bacteria also present in the sample. However, the current liquid culture methods rely on the effects of bacterial metabolism (changes in O_2/CO_2 levels, pH, etc.) to bring about measurable changes to the suspension. Hence, for slow-growing microorganisms like *M. tuberculosis* (*Mtb*), they take a long time (up to 6 weeks) to yield results.

To cut the time to positivity, we applied the detection concept of “detection by death” and using our high sensitivity microchannel Electrical Impedance Spectroscopy (m-EIS) method to detect bacteria in various samples rapidly. Viable bacterial cells can be killed in a few hours with very high doses of cidal drugs. m-EIS relies on the fact that high-frequency AC fields cause transient charge-accumulation at live cells' intact membranes. Cell-death in the microchannel causes charges to no-longer be accumulated, and the bulk capacitance of the microchannel will decrease. By picking up this change, we can rapidly detect viable bacterial cells in a testing sample.

For viable TB bacteria detection, we use synthetic sputum with gram-positive bacteria, gram-negative bacteria, and *M. tuberculosis H37ra*. After decontamination (kill all non-TB bacteria), we are able to discern decreases in bulk-capacitance for suspensions containing ~500 CFU/ml of Mtb cells (but not for ~50 CFU/ml). Thus, our turnaround-time (~4 hours) and limit-of-detection (<500 CFU/ml) are comparable to those of GeneXpert™.

Using our m-EIS method, we can also detect Lactic Acid Bacterial (LAB) contamination for ethanol fermentation with a low concentration of 5000 CFU/ml in less than 3 hours. Our detection of limit for LAB has a three-order reduction than the HPLC method, but with a similar detection time.

Aside from investigating the bacterial activities in the solution, we also observed the biofilm formation on the electrodes. We have observed that the interfacial capacitance also increases in proportion to the number of cells in the biofilm matrixes. In the future, we believe that we could also record cell death within biofilm using our method, and so researchers will be able to use it to screen new anti-biofilm material and drug rapidly.

CHAPTER 1
RESEARCH BACKGROUND AND MOTIVATION

Since humans first time directly observed bacterial cells[1], people started to fundamentally understand the mechanism of bacterial diseases caused by microbes' activities. Currently, many microbial detection methods have been developed directly or indirectly to detect microbial activities, including plate count method, light microscope, fluorescence imaging, and recent molecular-based techniques. All these detection methods have to consider some factors of detection limits, time to positivity, and the cost.

For bacterial disease diagnosis, the detection time is crucial. For example, even cutting 12 hours of detection time can decrease infection-related mortality higher than 20% for bloodstream infections[2]. Molecular methods can rapidly detect bacteria, find the bacterial ID, and perform limited drug susceptibility tests. Compared to other methods such as the liquid-culture method, however, it still has a much higher cost.

Due to low operational costs and rugged performance, liquid culture systems remain the workhorses for detecting pathogenic microorganisms, such as, food quality testing (Bactometer, RABIT, TEMPO, etc.), blood culture (BACTEC and BacT/Alert), and for detecting extremely slow-growing pathogens like *M. tuberculosis* (Trek ESP, MGIT, etc.). All liquid-based systems currently on the market rely on detecting living bacteria by looking for changes brought about by bacterial metabolism to the properties of the suspension (such as O_2/CO_2 levels, pH, electrical conductivity, temperature, etc.). The reason for long times to detection (TTDs) is that these techniques suffer from a fundamental limitation:

the amount of metabolite processed by an individual bacterium is extremely small.

Given that one bacterium (*E-coli*) consumes ~2 x 10^{-14} moles of O_2 / hr[3] and that a well-oxygenated sample has a dissolved O_2 concentration ~2x10^{-4} M (2x10^{-7} moles/ml), even if the sample has 1000 bacteria cells per ml to begin with, the per hour consumption of oxygen represents only a 0.0001% change in the O_2 level in the medium as a whole – a change so small that it is likely to be swamped out by "noise" in any sensor. Hence, with the current state-of-the-art systems, one has to wait for the bacterial concentration to rise to ~10^{7-8} CFU/ml before their metabolism can change the medium properties (O_2/CO_2 concentration, pH etc.) to a measurable degree[4]. In other words, they have an inherently high "threshold of detection" (the concentration at which the presence of living bacteria can be distinguished from the background). It further follows that any attempt to improve sensors for metabolites will at best lead to only marginal improvements to the TTD.

In contrast, our research group has developed (and patented [5]) a novel method to detect the presence of proliferating microorganisms in suspensions. It relies on the fact that in the presence of AC electric fields, the membranes of cells become polarized and store charge; thereby acting like electrical capacitors [6]. These capacitances at the individual cells contribute to the overall "bulk capacitance, C_b" of the suspension (net charge stored in the interior). The amount of charge stored by a live bacterium is about 100x that of an equal volume of aqueous solution[7]. Thus, even at low concentrations (volume

fractions), bacteria in a suspension contribute significantly to the latter's bulk capacitance.

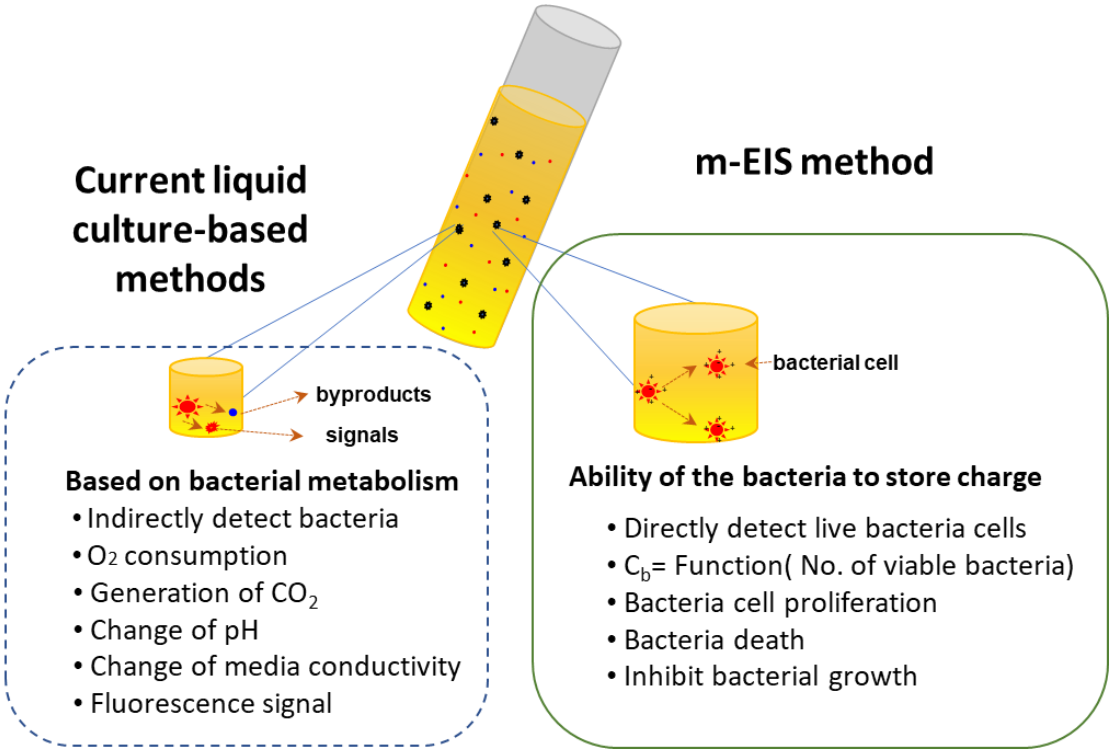

Figure 1.1 Liquid culture-based bacterial detection method. The current liquid culture-based methods detect bacteria by byproducts of their metabolisms. Our m-EIS based culture method directly detect live bacterial cells.

Our m-EIS method is fundamentally different from other methods that use electrical impedance to detect bacteria's presence. A large body of work exists in the food-safety area that detects changes to the electrical properties of the solution brought about by bacterial metabolism [8-10]. Viable bacteria break down sugars to more conductive species such as lactate and carbonate. This makes the solution more conductive, decreasing Bulk Resistance (R_b) [11] and total Impedance (Z) [12]. Interfacial capacitance (C_i) is also affected [13] since the ions on the surface are in electrochemical equilibrium with the bulk. There

exist instruments already commercialized (e.g., RABIT[14]) or under development [15, 16] that use these effects, but (like the BACTEC) their TTDs are fundamentally limited by bacterial metabolism rates. Until our work [17], others had failed to detect changes in C_b, although they had tried to measure it [18]. Our innovation has been to measure this usually neglected parameter, and show that by tracking it over time, we can detect viable bacteria in the sample directly and rapidly.

Based on the principles our detecting theologies and our previous testing results, m-EIS method has the advantages: (a) it is highly sensitive compared to current culture-based methods because C_b is strongly influenced by the presence of live bacterial cells [17]; (b) it is self-normalizing: Not like other detection techniques, m-EIS always has the a value of the initial reading of the bulk capacitance (C_b). Different samples may start out with varying initial values of C_b due to various reasons (E.g., the unalike initial load of bacteria, various ionic strength of media, size variation of the testing channels, etc.). We can, however, use the exact same criterion (significant increase or decrease of C_b from their respective baseline, such as 0-hr values) to determine the presence of viable bacteria in all cases. The "threshold" concentration (CFU/ml at which the suspension's C_b becomes significantly different from the baseline value) is various for different substrates, but has been found to be ~1000 CFU/ml (10 CFU per 10µL), in all samples we have tested thus far (bacterial growth media, food matrices, and blood culture media)[19-21]. The "thresholds" seen are shown in Table 1.1.

Table 1.1 Threshold concentrations recorded for different matrices (in CFU/ml), and its implications with respect to the performance of the proposed system.

Matrix	Apparent Threshold	
	CFU/ml	CFUs /10 µL
Milk	200	2
Apple Juice	100	1
Blood Culture	600-1000	6-10

Existing liquid culture-based methods, such as BACTEC, BacT/Alert, MGIT, etc., detect live bacteria indirectly: based on the metabolites that the bacterial cells consume/release as they grow/proliferate. As previously described, the EIS culture method is an improvement: in the sense that it detects viable cells directly based on the charge stored (and is able to achieve lower detection thresholds as a result), but it is still based on bacterial proliferation in the sense that it needs the bacterial cells originally present to go through a number of cycles (doublings) before their increased numbers can contribute measurably to an increase in the bulk capacitance of microchannel. In other words, it is still limited by how fast the cells proliferate. Thus, for extremely slow-growing microorganisms, such as *Mycobacterium tuberculosis*, times to detection remain unacceptably long.

To further cut the time to detection, we applied the idea of “detection by death”. The concept of “detection by death” rests on three insights: (1) that only living cells can be killed, (2) it is possible to kill any living cell much faster than it can grow (double), and (3) m-EIS allows us to pick up signatures of cell death since dead cells no longer store charge at their membrane interface and this leads to a decrease in the bulk capacitance of the cell suspension. We have applied this insight to rapidly (in < 6 hrs) detect the presence of live mycobacterial cells in (synthetic) sputum. Beyond that, we also realized that if the

killing agent was selective (in the sense that it killed only a certain type of cell among the different kinds present in a suspension), then this killing action could itself serve as a mechanism to detect the cells affected. We used this insight, and the fact that penicillin-class antibiotics kill bacteria, but not yeast to detect the presence of microorganism contamination in the bioprocessing process, such as lactic acid bacterial contamination in bioethanol fermenters.

Finally, a key aspect of the data analysis of m-EIS was out ability to tease apart the contributions of the bulk and the electrode-solution interface to the total measured electrical impedance. In the cases described earlier, the cells of interest were present in the bulk. However, in certain applications, the cells of interest may be located on an electrode surface. Here the basic approach of EIS could still be applied, with the minor modification of tracking the interfacial capacitance over time to check for cell proliferation.

Such a situation is encountered during the formation of biofilm. Biofilms are communities of microorganisms in which cells stick to each other and to a surface. These cells also secrete a slimy extracellular matrix composed of polysaccharides, proteins, and lipids. This matrix makes the bacteria lodged within it highly tolerant of antimicrobials. Biofilm-forming bacteria can adapt to their host immune responses, which causes a challenge for the patients to recover from chronic illnesses[22]. Biofilm forming microbes are supposed to cause higher than 60% of human infections [23]. So, there is a great demand for new anti-biofilm drug development and anti-biofilm material applications. By analyzing changes in the interfacial capacitance, we can study the biofilm

formation on electrode (made by the material where biofilm usually grows on) surfaces and use it to screen anti-biofilm materials and to study the efficacy of candidate anti-biofilm drugs.

In this thesis, there are five chapters. In the first chapter (this one) we state the research background and our motivation to focus on our chosen research topics. In the second chapter, we perform some theoretical studies regarding electrochemical impedance applications in detecting bacterial activities. In the third chapter, we apply our technique to rapidly detect *Mycobacterium tuberculosis* for clinical TB disease diagnosis. In the fourth chapter, we use our m-EIS based platform to detect lactic acid bacteria (LAB) contamination in yeast cultures that serve as inoculums for bioethanol fermentation. In the last chapter, we explored an innovative method based on the EIS technique to study bacteria biofilm formation on the surface of implant material and suggested using this method for antibiotic material screening and new anti-biofilm discovery.

CHAPTER 2
ELECTROCHEMICAL IMPEDANCE SPECTROSCOPY BIOSENSOR

2.1 Basics of electrochemical impedance spectroscopy

Ohm's law states that when a voltage (E) is applied across an electrical element, the current (I) that flows across it is directly proportional to the applied voltage, and the ratio of the applied voltage to the electrical current is known as resistance (R). When the voltage applied is a sinusoid (as in alternating current or AC supply), then the resulting current (while being proportional in magnitude to applied AC voltage) also may have a phase difference with the applied voltage (see figure 2.1). This combination of magnitude and phase is captured by the quantity known as "impedance".

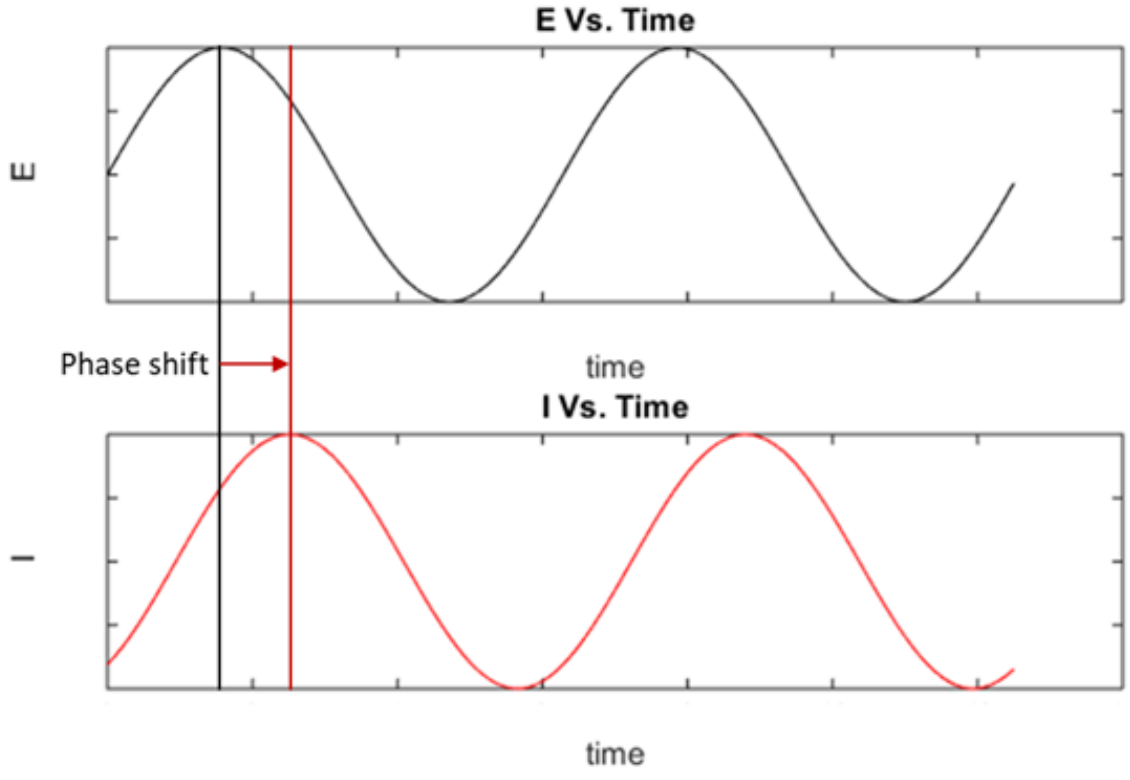

Figure 2.1 Sinusoidal current response in a linear system

Mathematically, the applied voltage signal has the form of

$$E_t = E_0 \sin(\omega t) \quad \text{eq 2-1}$$

where E_t is the electrical potential (voltage) at time t, E_0 is the amplitude of the signal, and ω is the radial frequency.

$$\omega = 2\pi f \quad \text{eq 2-2}$$

The response signal (the electrical current. I_t) has an amplitude I_0 , and is shifted in phase (Φ) with respect to the applied voltage.

$$I_t = I_0 \sin(\omega t + \phi) \quad \text{eq 2-3}$$

An expression analogous to Ohm's Law allows us to calculate the impedance of the system as:

$$Z = \frac{E_t}{I_t} = \frac{E_0 \sin(\omega t)}{I_0 \sin(\omega t + \phi)} = Z_0 \frac{\sin(\omega t)}{\sin(\omega t + \phi)} \quad \text{eq 2-4}$$

The impedance is therefore expressed in terms of a magnitude, Z_o, and a phase shift, Φ. With Eulers relationship,

$$\exp(j\phi) = \cos\phi + j\sin\phi \quad \text{eq 2-5}$$

the potential is described as,

$$E_t = E_0 \exp(j\omega t) \quad \text{eq 2-6}$$

and the current response as,

$$I_t = I_0 \exp(j\omega t - \phi) \quad \text{eq 2-7}$$

The impedance is then represented as a complex number.

$$Z_{(\omega)} = \frac{E}{I} = Z_0 \exp(j\phi) = Z_0(\cos\phi + j\sin\phi) \quad \text{eq 2-8}$$

The expression for $Z_{(\omega)}$ is composed of a “real” and an “imaginary” part, with the former representing the part of the impedance that is in-phase with the applied signal, and the latter representing the part that is out-of-phase. In a Nyquist Plot (see figure 2.2), the real part is plotted along the X-axis is the imaginary part is plotted along the Y-axis. Another presentation method and the Bode Plot (see figure 2.3). The impedance is plotted with log frequency on the X-axis and both the absolute values of the impedance ($|Z|=Z_0$) and the phase-shift on the Y-axis. Unlike the Nyquist Plot, the Bode Plot does show total impedance change and phase angle with the frequency information.

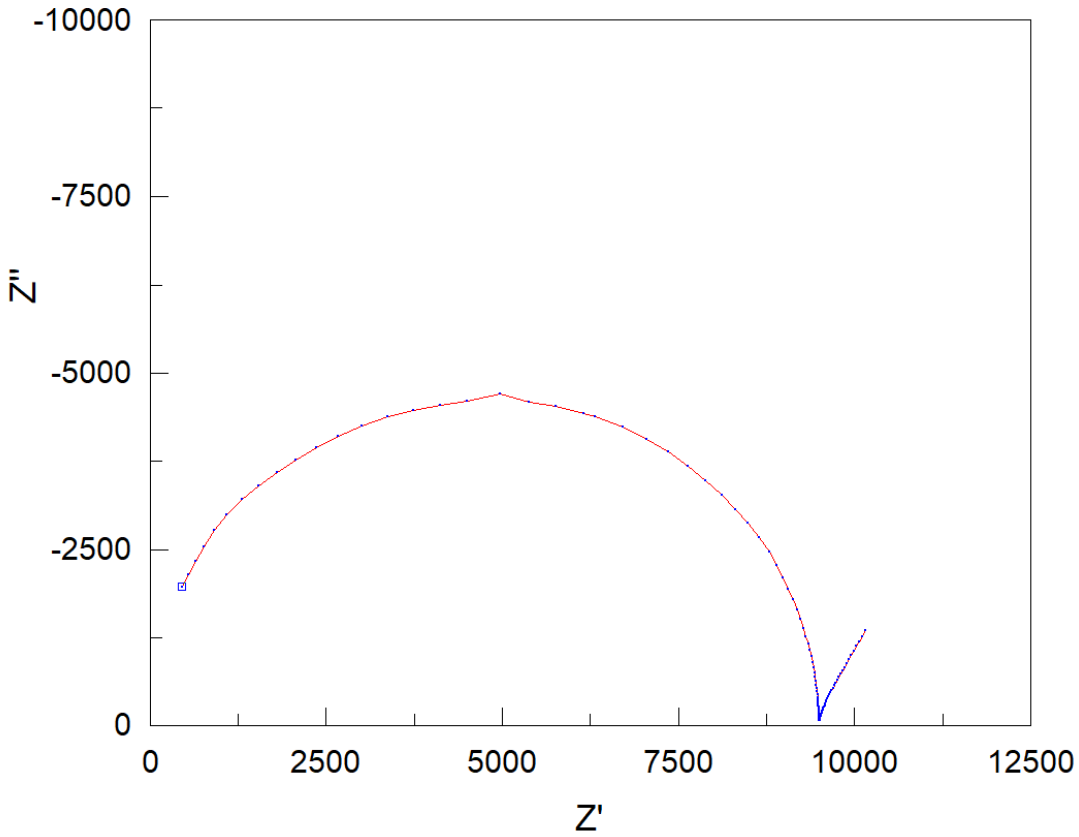

Figure 2.2 Nyquist plot with impedance vector

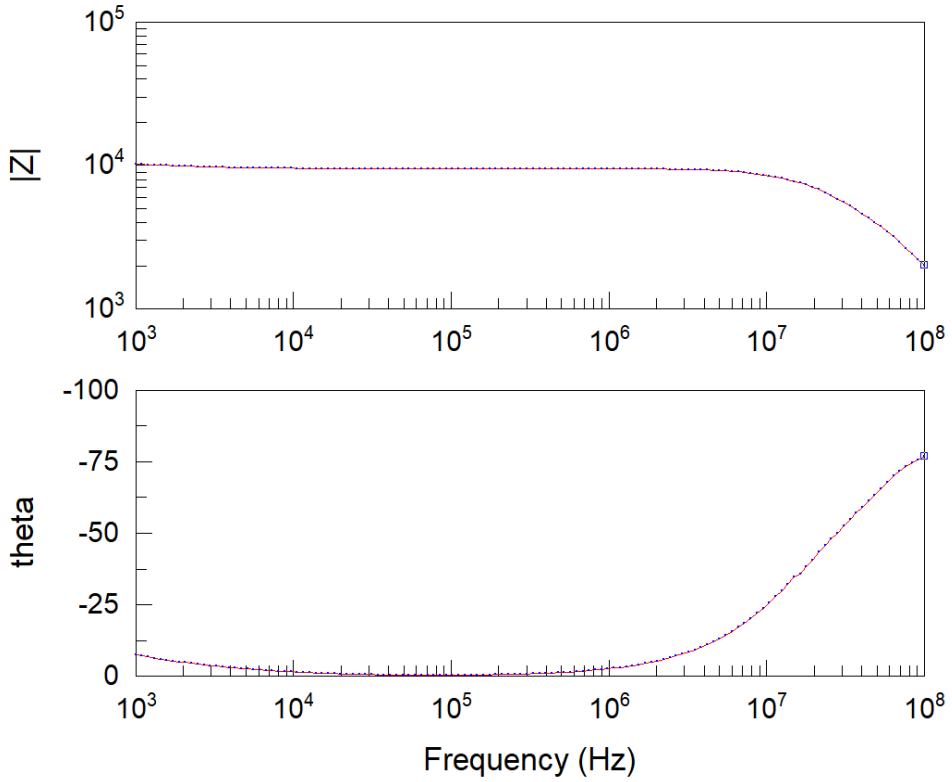

Figure 2.3 Bode plot with one time constant

2.2 Cell suspension in an electric field

Maxwell derived theoretical models for the behavior of spherical particles under an electric field and derived an equation (see eq 2-9) for a suspension of spherical objects[24].

$$\frac{\sigma_S^* - \sigma_e^*}{\sigma_S^* + 2\sigma_e^*} = P\frac{\sigma_P^* - \sigma_e^*}{\sigma_P^* + 2\sigma_e^*} \quad \text{eq 2-9}$$

Where, σ* is the complex specific conductivity, P is the fraction volume of the particle in the solution. S, e, and p denote the whole suspension, the external medium, and the effective particle conductivities, respectively.

With a low concentration of bacterial cells in the solution, say 10^4 CFU/ml concentrations of 2 μm sphere-shape bacterial cell, the fraction volume is about

10^{-8}. The fraction of the bacterial cell, P is $\frac{10,000 \times 4/3 \times \pi \times (1 \times 10^{-4} cm)^3}{1 cm^3} \approx 4^{-8}$.

From Maxwell's equation (eq 2-9), for a low concentration of bacterial cell suspension, the change of the impedance due to the cell proliferation is in sub-micron levels. This analysis suggests that to detect the impedance change due to the bacterial cells suspend in the solution. We need an impedance analyzer with a much less than micro-ohms precision. Meanwhile, it is well known that microorganism activities will change the solution properties, such as ionic strength, which can contribute to the background noise to swamp the "useful" signal of the bacterial cells generated. The other disadvantage of the volume frication equation is that the non-bacterial cell particles also contribute to the impedance change (see figure 2.4). It will cause a not actuate measurement especially low concentrations of bacterial cells that present in the solution.

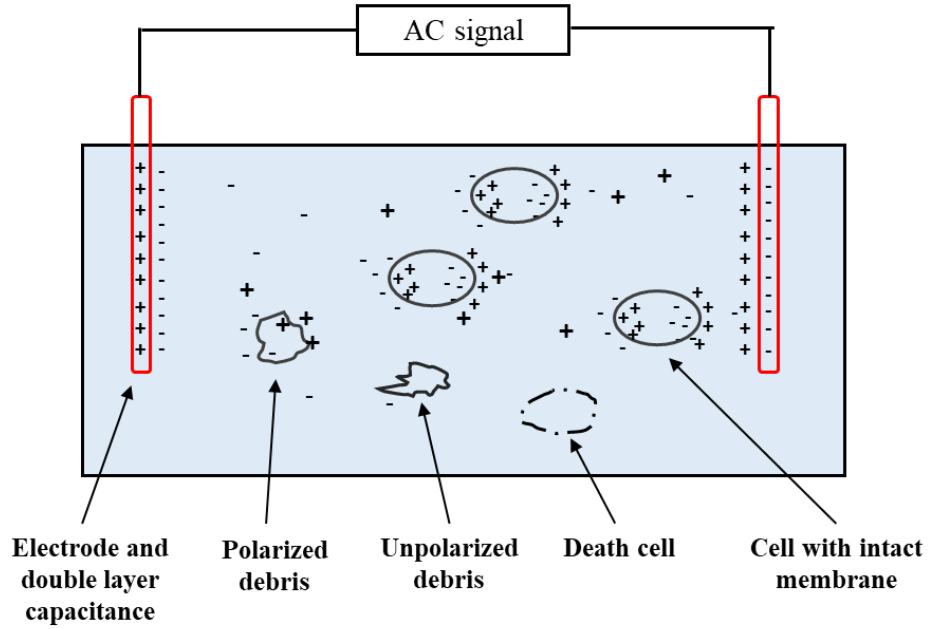

Figure 2.4 Cell suspension in a complex environment

Later, McClendon has developed an RC equivalent circuit method to study the cell suspension's impedance[25]. They measured the electric conductivity of blood and used the RC equivalent circuit method to analyze the electric impedance and reactance of blood to AC signals. Other researchers used the impedance data with an equivalent circuit to estimate membranes' thickness from a single planar bilayer's impedance measurements with accurate results[26].

Although the equivalent circuit method has been widely used to analyze the EIS measured data in many applications, it is still a challenge to measure the tiny changes in C_b of a cell suspension since C_e, interfacial capacitance on electrodes (see figure 2.5), is ~1000x larger than C_b. By employing the microchannels techniques in EIS, it enables us to detect changes in C_b, despite the "screening effect" of the charges at the electrode-solution interface (C_e)[17]. By placing the suspension in a long narrow microfluidic channel (see figure 2.5), we increase the effective bulk resistance of the suspension. This increases the bulk (R_b*C_b) impedance to be comparable to that of the interface at realizable frequencies, allowing an appreciable voltage to drop over the bulk-suspension. Thus, the charge-storage in the bacteria contributes significantly to the measured impedance.

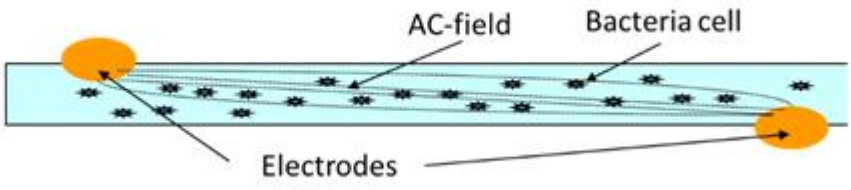

Figure 2.5 Cell suspension in an A.C. field. Bacterial cells play as tiny capacitors under an AC field

2.3 Cell suspension in a microchannel

In the long narrow microfluidic channel, an individual cell suspended in media, its membrane becomes polarized under the AC field. For lower frequencies, the membrane effectively insulates the cytoplasm, and the current can only flow around the cell (see figure 2.6(a)). The interaction between cell suspensions and the electric field is not significant. As the frequency increases and the cell membrane becomes more conducting (see figure 2.6(b)), the current flow begins to depend on the ratio of the complex conductivity of the cytoplasm to that of the bulk solution[27], which can be expressed in the eq2-9[28]. Because R_c (resistance of the cell cytoplasm) is couple order smaller than $1/(jwC_m)$ under the moderate-high frequencies (such as 1k-100M Hz for the cell suspension in a microchannel)[29], eq 2-9 can be rewritten for eq 2-10. For higher frequencies AC field is starting to penetrate the cell (see figure 2.6(c)). The interaction between cells in the solution and AC field is becoming lower. To analyze the cell suspension, the equivalent circuit, as shown in Figure 2.6 (d), can be used to fitting the impedance data in a Nyquist plot, as shown in figure 2.6(e) to extract the parameters of each component of the equivalent circuit for the cell suspension in a microchannel.

$$Z_b = \left(\frac{1}{R_m} + \frac{1}{R_c + 1/(j\omega C_m)} \right)^{-1} \quad \text{eq 2-9}$$

$$Z_b = \left(\frac{1}{R_m} + j\omega C_m \right)^{-1} \quad \text{eq 2-10)}$$

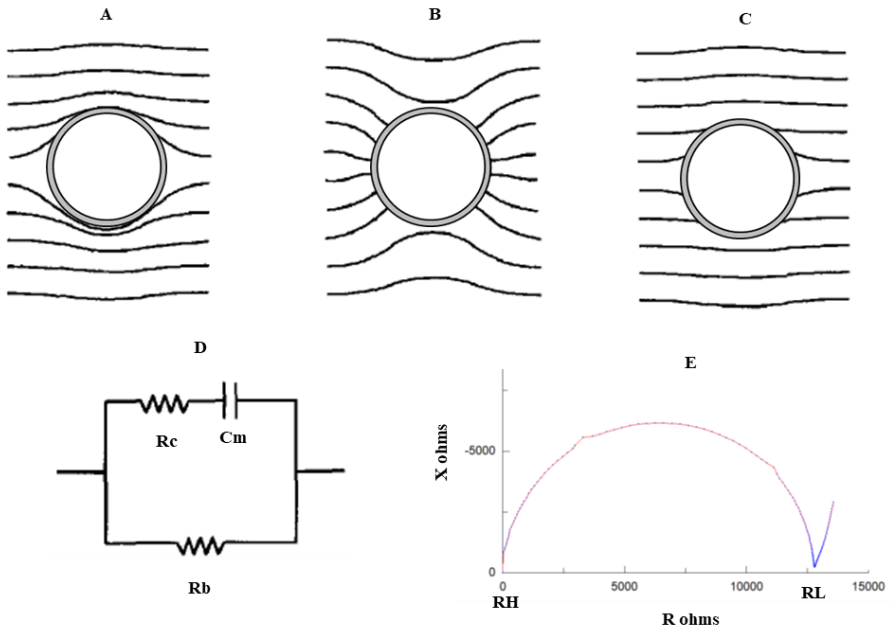

Figure 2.6 Interfacial polarization in cell suspensions. Lines of current flow around cell placed in a uniform A.C. electric field are shown for increasing frequency (a-c). (d) An equivalent circuit for a cell suspension. (e) A complex impedance plane representation, R vs. X, of cell suspension impedance.

As shown in figure 2.5, using an impedance analyzer to measure the impedance of the cell suspension in a microchannel, two electrodes will contribute to the total impedance. We modified the equivalent circuit model described in figure 2.6(d). A new model of the equivalent circuit, as shown in figure 2.7, which includes components of resistors (R_e) and capacitor (C_e) from electrodes, will be used to analyze the cell suspension in a microchannel. So, the microchannel's total impedance can be expressed in eq 2-11, where, C_b denotes the bulk capacitance of the microchannel and it the sum of C_m (membrane capacitance) and C_s (media solution capacitance); R_e denotes resistances of electrodes and C_e denotes interfacial capacitance on the surface of electrodes.

$$Z_{measured} = \left(\mathrm{R_e} + \frac{R_b}{1+\omega^2 R_b^2 C_b^2} \right) - j\left(\frac{1}{\omega C_{dl}} + \frac{\omega R_b^2 C_b}{1+\omega^2 R_b^2 C_b^2} \right) \quad \text{eq 2-11}$$

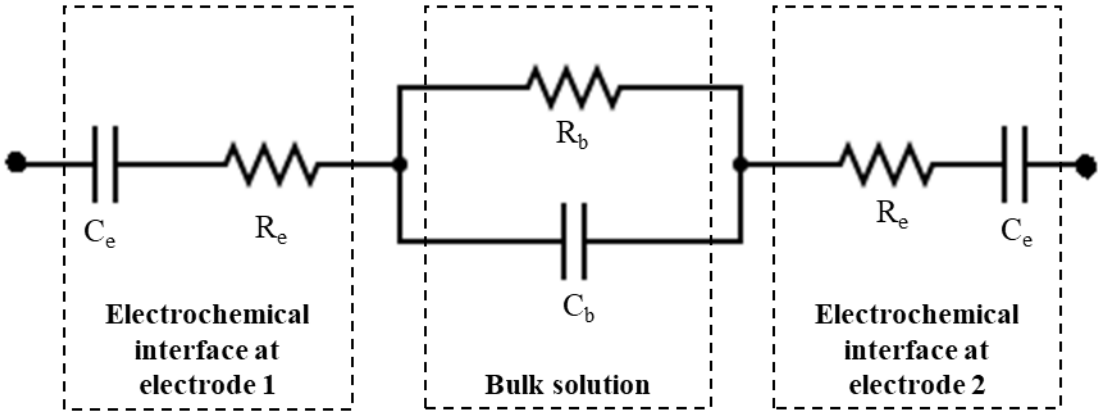

Figure 2.7 Equivalent circuit for cell suspension in a microfluidic channel

2.4 Interfacial capacitance

An electrical double layer occurs at the interface between an electrode and its nearby electrolyte, where ions and/or dipole molecules in the electrolyte change their position and alignment to weaken the electric effect field[30, 31]. Charges in the electrode's surface are separated from the charges of these ions and/or dipole to form an ultrathin layer of tenths of a nanometer[32]. The electrical double layer can be compared to the behavior of a capacitor in an electrical circuit. For a planar electrode, the interfacial capacitance is given by

$$C = \frac{\varepsilon_0 \varepsilon_r}{H} \quad \text{eq 2-12}$$

Where, ε_0 and ε_r denote the free space permittivity and the relative permittivity of the electrolyte solutions, respectively, and H presents the thickness the Helmholtz double layer, which can be approximated as the radius of solvated ions[32]. With a bare-metal immersed in an electrolyte, the value of interfacial capacitance is approximately 1-100 μF /cm^2 on an electrode's surface, which

depends on ionic concentrations, electrode potential, temperature, types of ions, oxide layers, electrode roughness, impurity adsorption, etc.[33, 34].

2.5 Cell growth on the surface of the electrode

A number of researchers have studied the impedance of electrodes in cell growth media. Giaever and Keese used electric fields to monitor cell behavior's dynamical aspect of tissue culture[34]. Later, they used this impedance method to monitor the cell morphology[35]. Other researchers have also employed interfacial layer change on the electrode to study cell behaviors based on the electrodes' impedance change where the cells grow[36, 37]. These previous works focus on the impedance of cell-covered electrodes.

Here, we want to investigate the situation of the interface of the electrode and cells that grow on its surface. As shown in figure 2.8, if there is cell growth on the surface of the electrode, the cell membrane will contribute to the value of the interfacial capacitance. Give that the surface of the cells will enlarge the total area of the electrodes. We hypothesize that due to the cell growth on the surface, the interfacial capacitance will increase. And, there will be a relationship between the cell density and the elevated value of the interfacial capacitance.

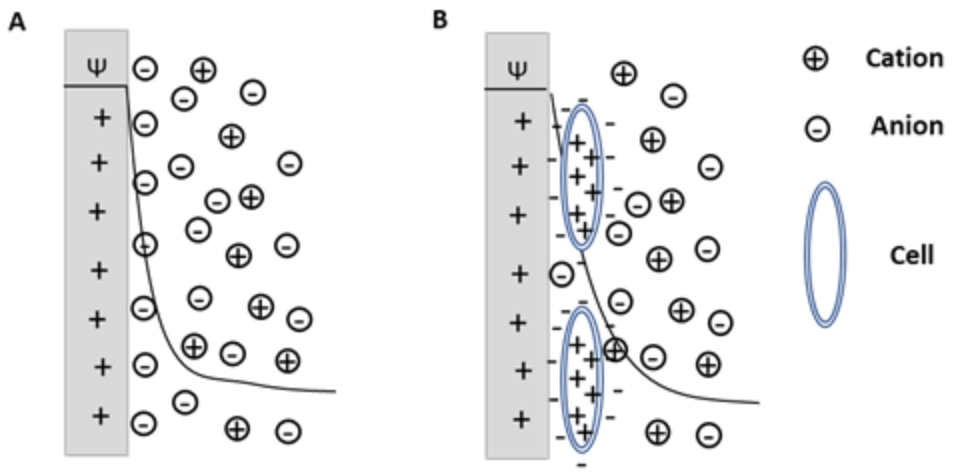

Figure 2.8 Interfacial layer on the electrode surface. a) Gouy-Chapman-Stern Model without cell growth on the surface. b) modified Gouy-Chapman-Stern Model with cell growth on the surface.

Interfacial capacitance values can be estimated by impedance analyzer and the impedance data can be analyzed using the equivalent circuit method to extract the cell growth information on the electrodes' surface. In this equivalent circuit as shown in figure 2.8, C_I is the interfacial capacitance, which consists of the series combination of the Helmholtz double-layer and the diffuse layer (see figure 2.9). Z_W is the Warburg impedance, is the charge-transfer resistance, and R_S is the spreading resistance. If cell growing on the surface, C_I will express the cell's information by look in for its values changing.

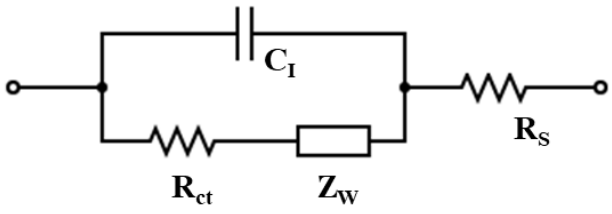

Figure 2.9 The equivalent circuit model for the interfacial of an electrode and solution.

CHAPTER 3
RAPID (< 6 HR) METHOD TO DETECT THE PRESENCE OF VIABLE CELLS OF *M. TUBERCULOSIS* IN SPUTUM, AS AN ALTERNATIVE TO LIQUID CULTURE

3.1. Introduction

Tuberculosis (TB) is a chronic disease with a high mortality rate. It is estimated that 1.5 million people died from TB in 2018[38]. One of the challenges in treating TB patients is the long duration of treatment with drugs, sometimes taking up to 24 months [39, 40]. During this long period, periodic sputum smear microscopy and/or sputum culture is often used to monitor the efficacy of the treatment protocol being used [41]. Results from these tests indicate whether there remain active (viable) TB cells in the sputum. Of these two techniques, sputum smear microscopy is inexpensive (appx. $2-10/test[42]) and can be performed at low resource areas. However, it has a relatively high limit of detection of ~10,000 CFU/ml. Hence, it is not very reliable in detecting the persistence of sub-populations of resistant cells, which may initially be low in number. On the other hand, the liquid culture of *Mycobacterium tuberculosis* (*Mtb*) using equipment such as the MGIT (Mycobacterial Growth Indicator Tube) system can, in theory, detect the presence of even 1 CFU of *Mtb* in the sample, but is relatively more expensive (appx. $12-60 /test[42]), requires reasonably well-equipped laboratories, and a long time to yield results. Samples must be kept in culture for six weeks (42 days) before they can be deemed negative.

The prevalence and spread of multi-drug resistant tuberculosis (MDR-TB) has made the issue of periodic monitoring more critical. In July 2018, the WHO convened a Guideline Development Group (GDG) to update its policy

recommendations for the treatment of MDR/RR-TB. For reasons such as better patient compliance and lower cost, the new guidelines [43] encourage wider adoption of short term (9-12 months) treatment regimens with orally administered drugs only, as opposed to longer (18-20 months) regimens and/or regimens that incorporate injectables as well. However, an important caveat is that the guidelines call for patients on both the short-term regimen and the longer-term regimen of oral medications alone to be monitored monthly using culture to ascertain the treatment's impact. It can switch to more aggressive regimens if *Mtb* continues to live/thrive in the face of the ongoing regimen. The long time needed to obtain culture results limits the ability to quickly detect a failing regimen and switch to a more aggressive treatment protocol. While molecular methods, such as RT-PCR (GeneXpert) can detect the presence of *Mtb* cells quickly (in ~3 hours) and have a low limit of detection (appx. 200 CFU/ml [44]), they are unsuited to monitor the decrease in the number of live cells[45, 46]. That is because recently death *Mtb* cells continue to be present in a TB patient's sputum, and DNA based testing is unable to distinguish such cells from live ones[46, 47].

We present here a method that can potentially meet all the needs of a system for monitoring the sputum of patients undergoing treatment for the continued presence of live *M. tuberculosis* (*Mtb*) cells, viz. an ability to detect live cells only (no false positives from dead cells) with low limits of detection, rapid time to results, and low cost with rugged performance. Our method is specifically designed to exclude dead *Mtb* cells, and its performance metrics such as limit of

detection (~500 CFU/ml) and turnaround time (< 4 hours) are comparable to molecular techniques such as the GenXpert. Moreover, we also believe that it has the potential of being low-cost and of capable of being performed at limited-resource locations such as regional clinics.

As discussed earlier, in our case, it is important that we report the presence of live cells, and not dead ones. The traditional approach to detecting live cells only in a sample that may also contain dead cells is to look for things that cells do when alive, such as consuming O_2, generating CO_2, changing the pH of the media around it, producing/consuming certain "marker" metabolites, or even producing m-RNAs (either in general, or of a particular type). The time to detection (TTD) of these detection techniques is hence limited by how fast the target cells produce/consume the tracked metabolites. Since *Mtb* has a low rate of metabolism/growth, such techniques take a long time (E.g. Up to 6 weeks for MGIT, which relies on detecting O_2 consumption[48]). Our approach, on the other hand, starts with the realization that there is one additional thing that live cells can do that dead cells cannot: DIE (you cannot kill a cell that is already dead, again). More importantly, cells can be killed much faster than they can grow (or produce/ consume detectable levels of tracked metabolites), and thus times to detection based on cell-death are likely to be much faster, and independent of the metabolic rate (doubling time) of the species of interest.

We have previously developed a way to monitor cell-death in near real-time using microchannel Electrical Impedance Spectroscopy (m-EIS)[49, 50]. Briefly, m-EIS relies on the fact that exposure to high-frequency AC fields leads to

transient charge accumulation at the intact membranes of living cells. Various mechanisms in cell necrosis lead to permeabilization/destruction of the cell membrane and this in turn, causes charges to no-longer be accumulated at the membranes. This effective loss of charge storage (capacitance) at the cell membranes is picked up using m-EIS. In earlier work[51], we have shown that using this "detection by death" approach, we were able to detect the presence of ~$5x10^5$ CFU/ml of both rapidly-growing *M. smegmatis* (doubling time of appx 3 hrs[52]) and the much slower-growing *M. bovis BCG* (doubling time of appx. 20 hrs [53]) in synthetic sputum in < 5 hours.

In this work, we try to gauge the potential of this technique to monitor the presence of live *M. tuberculosis* cells in the sputum of TB patients undergoing treatment. To do so, we try to estimate the limit of detection for *M. tuberculosis* cells in sputum, and the turnaround time for the user to obtain results. We foresee our test to proceed as follows: First, 2-5ml of sputum is to be collected from test-subjects. Next, this sputum is to be decontaminated using standard protocols, typically involving Sodium Hydroxide and N-Acetyl-l-Cystein (NaOH-NALC). Then, per instructions in a sample processing kit, antibiotic(s) are to be added to the decontaminated sputum, and the processed sputum is to be loaded into a microfluidic cassette containing one or more microchannels with electrodes attached. The cassettes are then to be inserted into a "card reader" unit that has electrical pads that connects the electrodes on the card to a circuit that can perform m-EIS measurements. The card reader is also expected to keep the card(s) at the optimal temperature that facilitates *M. tuberculosis* cells'

metabolism. One or more card readers can be connected to an inexpensive data processing unit (computer/ tablet/ phone) that houses software to analyze raw-m-EIS data, track computed parameters over time and interpret results. It is expected that after about 3 hours of incubation, the card reader will indicate (based on near real-time analysis of the m-EIS data) whether live Mtb cells were present in the sputum samples tested.

3.2. Materials and methods

3.2.1 Rationale for the approach

The purpose of this work is to demonstrate proof of principle. For the proposed method to work, (a) the *Mtb* cells present (or at least a significant fraction) must be killed off by the added antibiotic within the period of observation (<3 hours), (b) the m-EIS method should be able to detect the cells' death in the presence of potentially interfering substances in the sputum (including both macromolecules and existing dead bacterial cells). Further, we wish to evaluate the load of live cells below which the cell-death signals will be lost in the background (the limit of detection). To achieve these goals, the following experiments were conducted.

3.2.2 Outline of the experimental protocol

Figure 3.1 shows a schematic of our experimental protocol. As depicted in figure 3.1(a), a synthetic sputum sample was prepared using established protocols [51]. To prepare synthetic sputum, aliquots from individual subcultures of gram-positive bacteria (*S. aureus* ATCC 29213), gram-negative bacteria (*Pseudomonas aeruginosa* ATCC 7853), and *Mycobacterium tuberculosis H37ra* (ATCC 25177) were added to mimic the presence of commensal and pathogenic

bacteria. The concentrations of *S. aureus* and *P. aeruginosa* in the synthetic sputum were ~10^5 CFU/ml for all samples created. The concentrations of *M. tuberculosis H37ra* ranged from ~50 to ~5x10^5 CFU/ml, along with an additional sample that had no *M. tuberculosis* cells. Then, as shown in figure 3.1(b), the synthetic sputum was subjected to decontamination and decongestion using Sodium Hydroxide and N-Acetyl-l-cystein (NaOH-NALC) using an established protocol[54]. This treatment kills all the non-TB microorganisms while leaving the *Mtb* cells alive. It also greatly decreases the viscosity of the sputum. After allowing the decontamination solution to act for 10 min, the reaction is quenched by adding 1x PBS solution. The diluted decontaminated sputum is centrifuged (as shown in figure 3.1(c)) to collect all the bacterial cells and resuspended in 7H9 media. Then, as depicted in figure 3.1(d), a high dose of Amikacin (32µg/ml) is added, and ~20µl of the sample is loaded into a microfluidic channel and monitored using m-EIS for the next 3 hours. As depicted in figure 3.1(d), if live *Mtb* cells were present at the end of the decontamination, they will now be killed. The bulk capacitance value obtained from m-EIS measurements (which reflects the amount of charge stored at membranes of living cells) will show a drop from the baseline (time t=0) value. If no living *Mtb* cells are present, then a flat line will be observed. Details of individual steps is provided below.

.

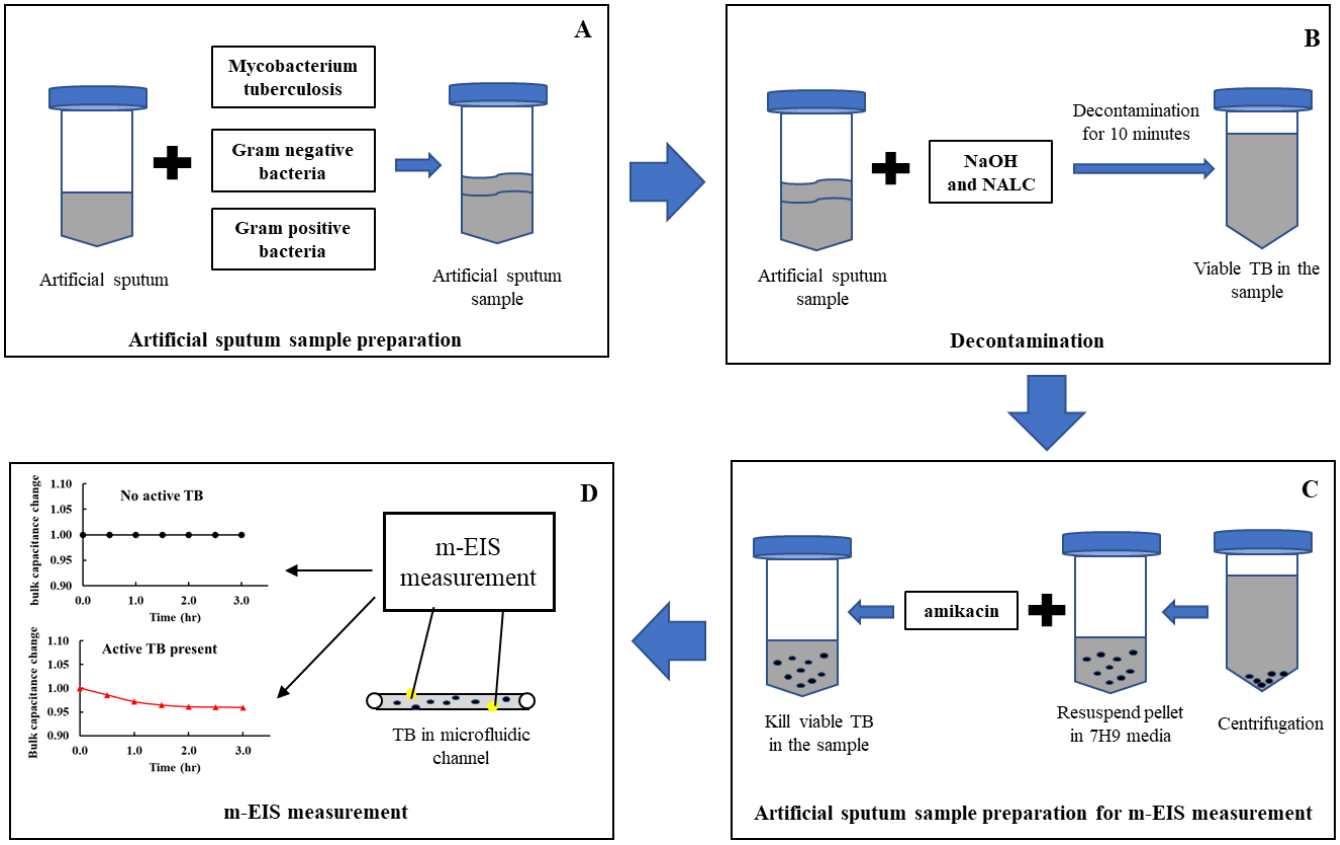

Figure 3.1 Schematic outline of the experimental protocol (a) an artificial sputum sample is prepared by spiking *Mtb* and other non-Mtb bacteria. (b) The synthetic sputum sample is decontaminated and decongested using NaOH-NALC solution (*Mtb* cells survive, but all other microorganisms are killed). (c) The decontaminated sputum is centrifuged, the pellet resuspended in 7H9 broth, Amikacin added (32 µg/ml) to kill living *Mtb* (if present) (d) sputum processed as above inserted into a microfluidic channel and m-EIS measurements taken periodically over the next 3 hours. Killing of *Mtb* cells by the high-dose Amikacin (and hence the presence of live *Mtb* cells) is inferred if bulk capacitance (C_b) values (calculated by analyzing the m-EIS data) decrease significantly during this period.

3.2.3 Preparation of bacterial cultures.

Mtb was sub-cultured in Middlebrook 7H9 media supplemented with Middlebrook Albumin Dextrose Catalase (ADC) supplements at 37 °C for a period of 1-2weeks. *S. aureus* and *P. aeruginosa* were sub-cultured in Tryptic Soy Broth (TSB) at 37 °C for 12 hours. The concentrations of *Mtb* and non-Mtb bacteria in these cultures were estimated using optical density measurements according to our previous tests[51, 55], and confirmed by plating on 7H9 or TSA plates, respectively.

3.2.4 Preparation of synthetic sputum and decontamination

The synthetic sputum was prepared by adding 10 grams of methylcellulose was added to 1 liter DI water, and the aqueous solution was autoclaved to make it sterile. Then, one emulsified fresh egg was added to the solution to make the artificial sputum. 5 µl of stock suspensions of *S. aureus* and *P aeruginosa* (obtained as described in the previous section and containing ~10^8 CFU/ml) were added to 5 ml of the synthetic sputum to achieve concentrations of ~10^5 CFU/ml, respectively. In addition, appropriate amounts of similarly obtained stock suspensions of *M. tuberculosis* were also added to produce synthetic sputum with ~50 CFU/ml, ~500 CFU/ml, ~5,000 CFU/ml, ~50,000 CFU/ml, and ~500,000 CFU/ml of *Mtb*.

Then, synthetic sputum was next subjected to decontamination and digestion using the standard NaOH-NALC process described in the literature[51, 54]. Briefly, 5 ml of synthetic sputum is taken, to which 5 ml of a solution of 2% Sodium Hydroxide and N-acetyl-L-cysteine (NaOH-NALC) is added to decontaminate and decongest the sputum. The NaOH-NALC solution kills all

non-Mtb cells while allowing the *Mtb* cells to survive, and simultaneously reduces the viscosity of the sputum. After letting the system stand for 10 minutes, 20 ml of 1X PBS (Phosphate Buffered Saline) is added to quench the decontamination process. The dilute decontaminated sputum is centrifuged (as shown in Fig.1(c)) at >3000g for 15 minutes, and the pellet is resuspended in 5 ml of fresh 7H9 growth media.

3.2.5 m-EIS measurement and data-analysis.

To 5 ml of the resuspended pellet suspension, 100 µl of a 1600 µg/ml stock solution of Amikacin is added to obtain a suspension with 32 µg/ml of Amikacin. This suspension is assayed for the presence of live *Mtb* cells by periodically injecting small (20 µL) aliquots of it into a microchannel for m-EIS measurement. This microfluidic cassette consists of a 3D printed Poly methyl methacrylate (PMMA) top and a glass-slide base, joined together using a biocompatible epoxy (Epo-Tek 301^{TM}, USA). It has microchannels of cross-section 1mm x 1mm, with electrodes asymmetrically placed 10mm apart, as shown in figure 3.2(c). It thus allows the user to assay a fluid volume of ~10µL (~10mm length x 1mm width x 1mm height) between the two electrodes in the microchannel. The resuspended pellet suspension with antibiotic was maintained at 37°C by placing it in an incubator. Periodically (once every 30 minutes, for 3 hours), it was taken out of the incubator for ~5 minutes, and five aliquots of 20µL each were introduced into the microchannels described earlier. Two electrodes in each microchannel were connected to an impedance analyzer (Agilent/Keysight 4294A), and m-EIS measurements were conducted.

The m-EIS method has been explained in detail in our prior work[19]. Briefly, m-EIS relies on the fact that exposure to high-frequency AC fields leads to transient charge accumulation at the intact membranes of living cells. While this charge accumulation, which takes place in the interior of the suspension (and is hence referred to as "bulk capacitance" (C_b)) is much (>100x) smaller than the charge that accumulates at the electrode-suspension interface (the "electrochemical interfacial capacitance" (C_e)), one is able to obtain estimates of the former by placing the solution in a thin-long channel, which increases the effective bulk resistance (R_b) of the suspension. This increases the impedance of the bulk ($=R_bC_b$) to be comparable to that of the interface ($= R_eC_e$, where R_e is the electrode resistance) at realizable frequencies (10 kHz to 100 MHz), allowing an appreciable voltage drop over the bulk-suspension. Thus, when C_b changes, so does the measured impedance.

The m-EIS method can accurately estimate C_b by using the Impedance Analyzer (Keysight / Agilent 4294A) which sends out 500mV AC voltage signals, and measures both the in-phase and out-of-phase components of the electrical impedance, Z, [the resistance (R) and the reactance (X)] at 201 frequencies (ω) ranging from 10 kHz to 100 MHz in rapid succession. The Z (R and X) vs. ω data from each scan is fitted to an equivalent electrical circuit shown in figure 3.3 using a commercially available software package (Z-view™ from Scribner Associates). The software provides an estimate for the various circuit parameters. Of these, the bulk capacitance (C_b) of the cell suspension, is tracked

over time to determine if cell-death is observed, and hence to indicate if viable *Mtb* cells were present in the sputum sample.

To determine if a significant change (decrease) occurred in the value of the bulk capacitance (C_b) at any given time (t) when compared to its baseline (value at t = 0), we use the Mann-Whitney U test. The U test is non-parametric test that compares the population average between two groups and tells if they are significantly different or not. We chose to use it instead of more popular tools like *t* test since we have only a few (5) data points (bulk capacitance readings) per time point and because the normality assumption of the reading which is required for a *t*-test is not appropriate for our data.

For any given sample, the values of C_b at each point in time (t) (5 readings each) are compared to those at t=0, and the U values corresponding to a p value of 0.05 (level of significance of 5%; two tailed test) are calculated. Our null hypothesis is that the two sets of C_b values are equal, with the alternative being that there is a significant difference between them. If the calculated U-value is equal to or lesser than the critical U value (2 in this case, since we have 5 readings at each time point)[51], then the null hypothesis is rejected. For a given sample, if 2 or more C_b values at consecutive points in time are found to be significantly lower than the baseline C_b, we conclude that there had been some viable cells present at t=0 that were killed during the experiment.

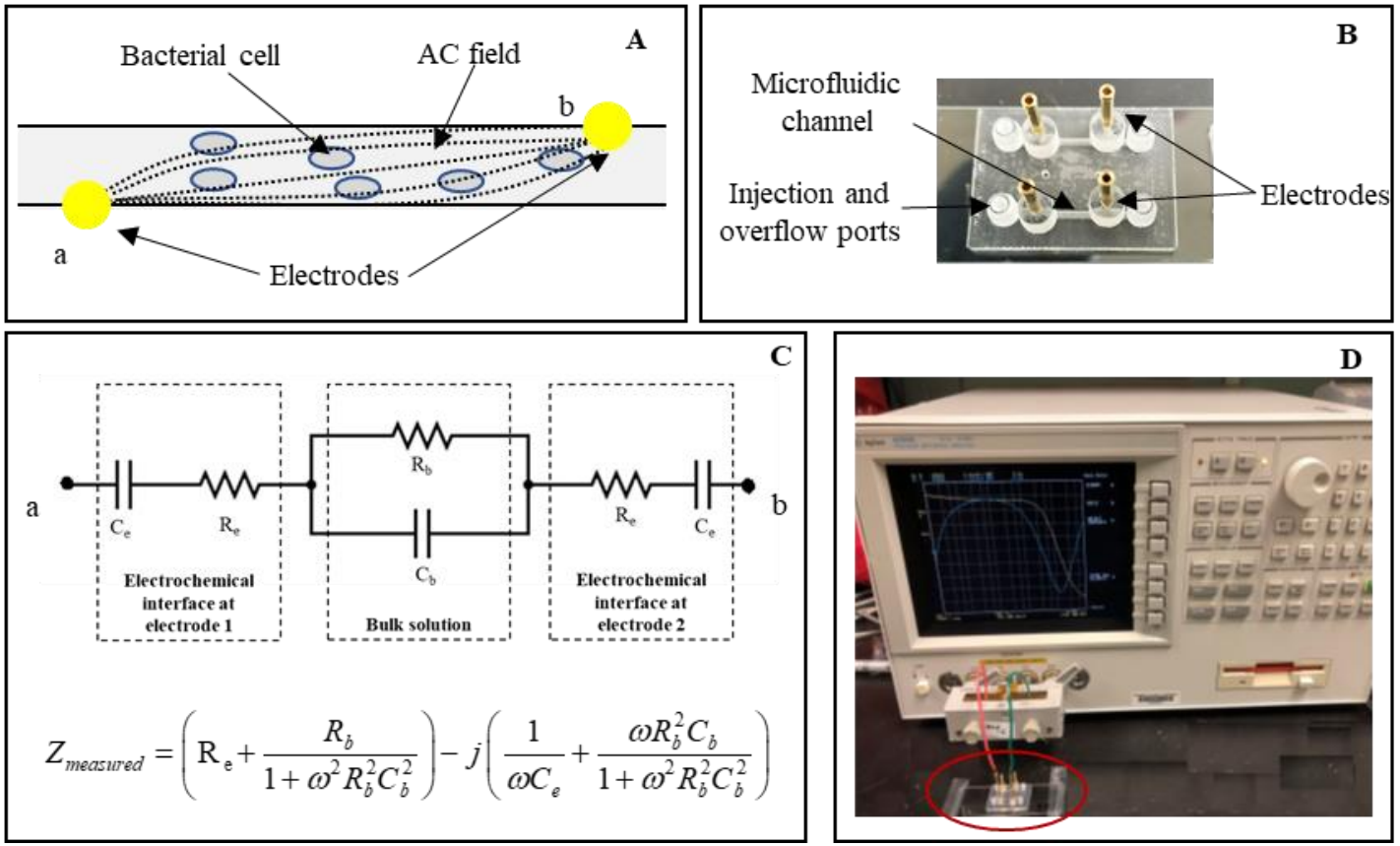

Figure 3.2 The m-EIS method (a) schematic of bacterial cells exposed to an AC filed in a microfluidic channel. (the channel geometry enables the electrical “lines of force” to interact more strongly with the bacteria) (b) a 3D printed microfluidic cassette with 2 long narrow channels and post electrodes placed asymmetrically (c) the equivalent circuit for microchannels and impedance equation, where C_b denotes the bulk capacitance of the microchannel; R_e denotes resistances of electrodes; C_e denotes the electrochemical interfacial capacitance, and R_b denotes bulk solution resistance. (d) the impedance of the fluid in a microfluidic channel (cassette inside the red circle shown) is scanned using an impedance analyzer.

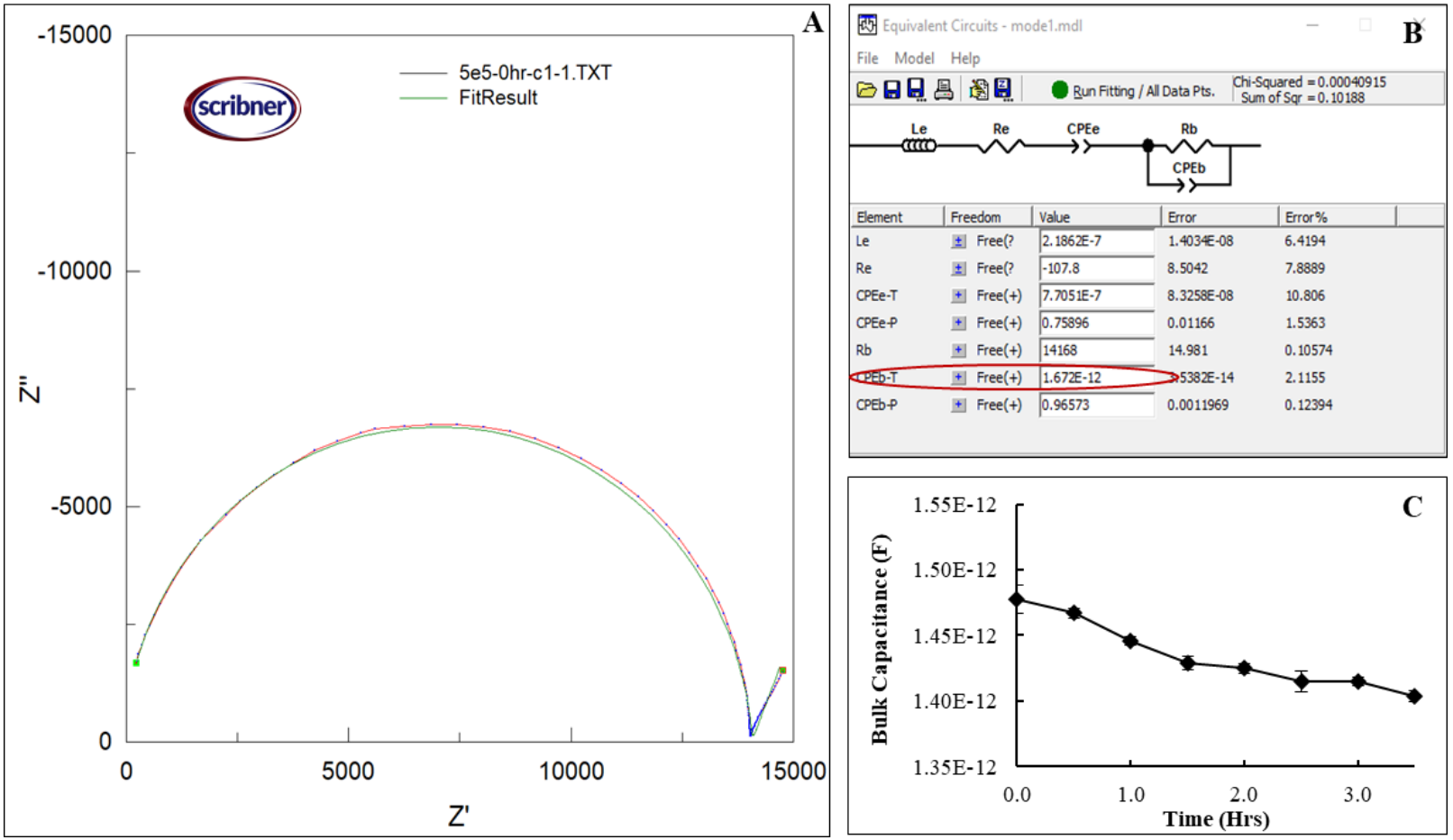

Figure 3.3 m-EIS data analysis by using the program Zview™ (a) graphical fit-line to the Nyquist plot, where Z' (x-axis) is resistance and Z'' (y-axis) is reactance. (b) the equivalent circuit is used to make the fitting for the Nyquist plot and extract the values of the circuit's components. (c) decreasing values of bulk capacitance (C_b) indicates cell-death due to the action of the antibiotic, and hence allows us to infer the presence of the viable *Mtb* in the sputum sample.

3.3. Results

Our results, for synthetic sputum samples with ~10^5 CFU/ml each of *S. aureus* and *P. auriginosa*, and with *M. tuberculosis H37ra* ranging in concentration from ~50 to ~500,000 CFU/ml (along with a sample that contains no *M. tuberculosis* cells), are listed in Table 1 and shown graphically in figure 3.4. Since microfluidic cassettes are assembled by hand, there is variation between individual cassettes. To account for these variations, all the data (Cb(t)) is scaled to their respective baselines ($C_b(t=0)$).

As was expected, the control (no bacterial cells of any kind) did not show any significant decrease in C_b over the course of the experiment, and neither did the sample with *S. aureus* and *P. aeruginosa* but no *Mtb* (0 CFU/ml *Mtb*). On the other hand, we are able to discern a significant decrease in the C_b values for samples with initial loads of ~500, ~5000, ~$5x10^{4,}$ and ~$5x10^5$ CFU of *M. tuberculosis* per ml of sputum. However, we failed to detect the anticipated significant decrease in C_b for the sample with an initial load of 50 CFU/ml. This implies that the limit of detection of this technique lies somewhere between 50 and 500 CFU/ml.

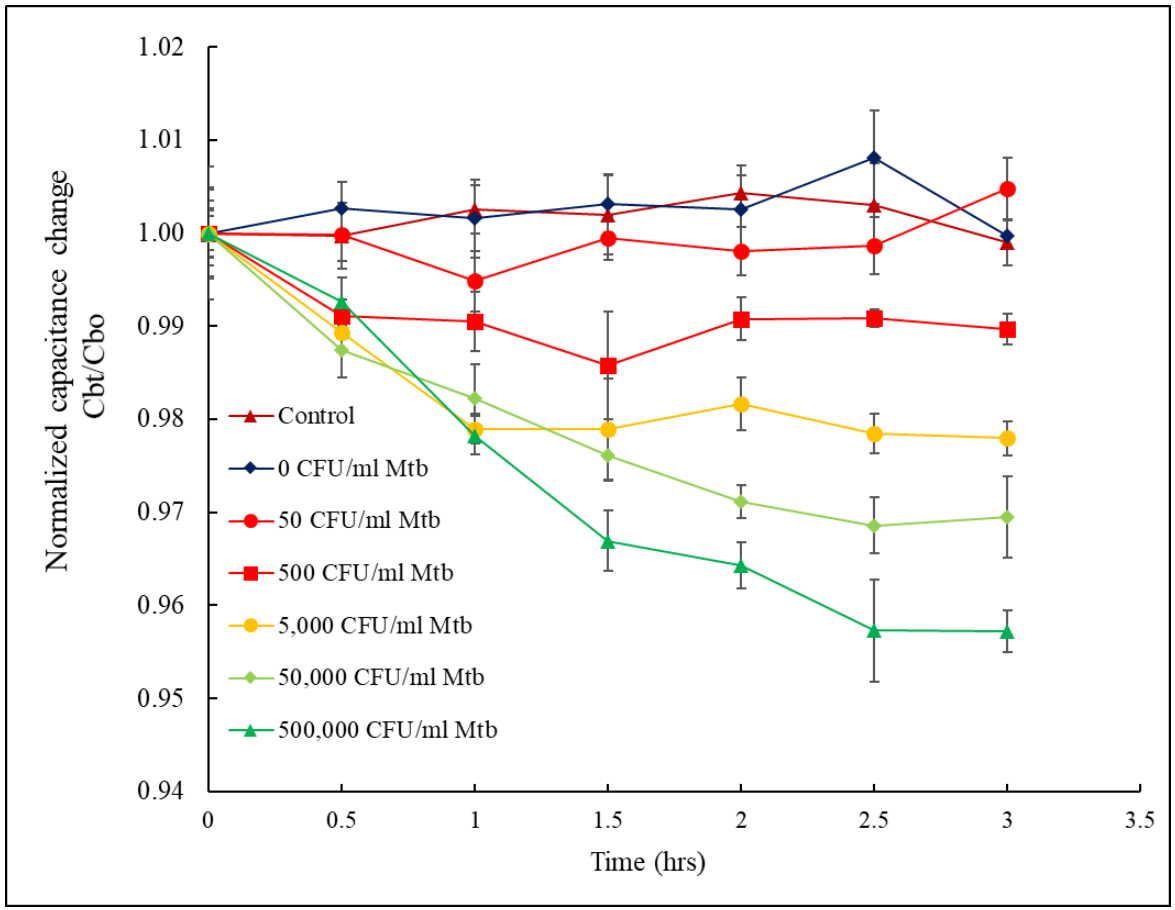

Figure 3.4 Scaled values of the bulk capacitance [C_b / C_b (t=0)] values as a function of time for synthetic sputum samples with different loads of *M. tuberculosis* cells, when exposed to Amikacin at 32 µg/ml. All C_b values are normalized to the mean of the respective baseline (t=0hr) reading (n=5 at each data point).

3.4. Discussion

The purpose of the work we present is to demonstrate that, using our m-EIS technique in the "detection by death" mode, it may be possible to ascertain whether a sputum sample contains live *M. tuberculosis* cells within a few hours (on the same day), as opposed to weeks currently taken. Doing so would, as explained earlier, greatly help in quickly adjusting failing treatment protocols. Our initial results (those presented here) are thus quite encouraging since they indicate that it may be possible to detect a load of <500 CFU/ml in the desired period.

We appreciate that the present study has many limitations, and much additional work needs to be completed before it can emerge as a technique that can be adopted in real-world settings. First off, we used synthetic sputum for this study. Real-world sputum is likely to have a large variability, whose effect on the sensitivity of the measurement cannot be predicted with absolute certainty. Nevertheless, we note that the protocol we used for decontamination and decongestion (digestion) of the sputum is routinely used for sputum samples obtained in clinical settings throughout the world, including sample prep before culture-based detection of *M. tuberculosis* using the MGIT^{TM} or similar systems. We hence expect to be still able to harvest live *M. tuberculosis* cells from real-world sputum. Our m-EIS method has also been shown to be effective in tracking the growth of cells in samples ranging from relatively clear liquids such as milk and apple juice[56] to complex fluids such as blood culture broth that contains > 10^7 red blood cells/ml (whole blood diluted 30-fold)[57], with thresholds of detection (concentrations where one can discern increasing cell numbers from

the background) of ~1000 CFU/ml or lower. We are hence not only fairly confident that we can achieve similar limits of detection when using real-world sputum, but we expect to further improve on this limit my making adjustments to the sample pre-treatment protocol and by optimizing the design of the microfluidic cassette to deal specifically with sputum samples.

In the protocol that we used, we re-suspended the pellet of microorganisms and other debris from the sputum in a volume of 7H9 medium that was equal to that of the original sputum (5ml each). If the pellet had been re-suspended in 0.5ml (500µl) of 7H9 medium instead, the limit of detection would have been reduced from the current ~500 CFU/ml to ~50 CFU/ml of sputum (which would make the limit of detection lower than that of the GeneXpert). A major reason for resuspending the pellet in the larger volume was to have enough suspension to conduct the repeated measurements at each time point over the observed duration of study. In future, we hope to have a microfluidic cassette with antibiotic(s) present in a lyophilized form within the micro-channel (similar to systems such as the VITEK used for antibiotic susceptibility testing). Like with the VITEK, we envision the card to filled just once and monitored continuously over time. With more frequent monitoring (say every 5 minutes, instead of every ½ hour as currently done), one could potentially obtain better statistics to discern even smaller changes than done in this study. The microfluidic card could also have multiple channels that could house multiple antibiotics and make the system more clinically sensitive and specific.

Another parameter that we foresee us having to optimize is the identity and concentration of the antibiotic(s) we use to kill the viable *M. tuberculosis* cells. That is especially pertinent given that we foresee this test being used for patients infected with multi-drug resistant TB. In this context, one must note that when an infecting strain is "clinically" resistant to a drug, it does not mean that the drug in question cannot kill the strain *in vitro* even at a high concentration. All it means is that *in vitro*, the Minimum Inhibitory Concentration (MIC) of the drug is higher than a certain agreed-upon cutoff value (breakpoint value). The cutoff value is decided upon based on correlations between *in vitro* values of MIC for the organism and clinical responses observed in the past. A MIC value higher than the breakpoint indicates that treating the patient with the drug is unlikely to be successful. For instance, the CLSI (Clinical and Laboratory Standards Institute) recommends a 1µg/ml cutoff value for Amikacin. Thus, a strain with an MIC of 2 ug/ml would be considered clinically resistant to Amikacin but would likely still be killed off rapidly using our chosen concentration of 32 µg/ml. Other bacterial cidal drugs, including relatively new ones such as Delamanid (Dlm) and Bedaquiline (Bdq) also show similar behavior (as shown in figure 3.5). The final product could either include a blend of different antibiotics or different antibiotics placed in different channels. In the latter case, a "positive" response from any one of the channels (significant decrease in C_b) would suffice as an indicator for the presence of viable *M. tuberculosis* cells in the sputum sample.

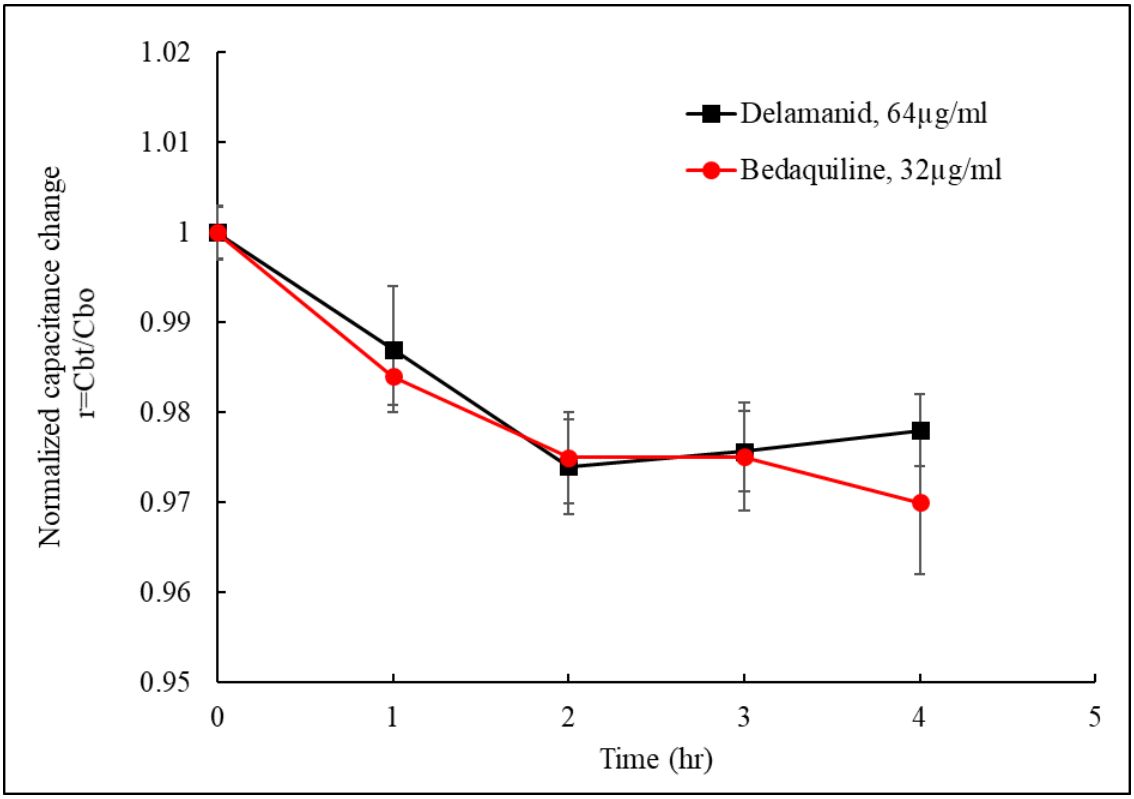

Figure 3.5 Delamanid (Dlm) and Bedaquiline (Bdq) can be used to kill viable Mtb cell. Dlm and Bed can kill *Mtb* in 2 hours and cause the bulk capacitance to decrease (*Mtb* is ~5x10^5 CFU/ml and n=5 at each data point).

The other issue we foresee potentially affecting the clinical specificity of this test is the incomplete decontamination of the sputum due to user errors such as over-dilution of NaOH or not allowing enough time for the NaOH-NALC solution to act. This is liable to yield false positives since the remaining non-TB bacterial cells are also likely to be killed by the Amikacin (or other antibiotics used). The solution to this problem can be achieved in one of 2 ways. The first way would be to also plate an aliquot of the decontaminated sputum in Tryptic Soy (or similar generic growth media) agar. Any surviving gram-positive or gram-negative bacterial would grow overnight (or within a couple of days), tipping off the clinicians to the possibility of wrong results. The other is by running our test on

another channel, with carbenicillin as the antibiotic. Carbenicillin is an antibiotic that does not affect *M. tuberculosis*, but kills most other gram-positive and gram-negative bacteria, and is hence used as an additive in TB culture broths to suppress contaminants [51]. As shown in figure 3.6, an inadequately decontaminated sputum (where the decontamination reaction was done with a lower concentration of 1% NaOH for 1 minute instead of 2% the recommended for 10 minutes), yields a signature of death (decreasing C_b) when exposed to 25µg/ml Carbenicillin, but an adequately decontaminated sputum does not. Hence, monitoring the response to carbenicillin (in addition to that of the other cidal antibiotics) can serve as a quality-control cross-check for the overall test.

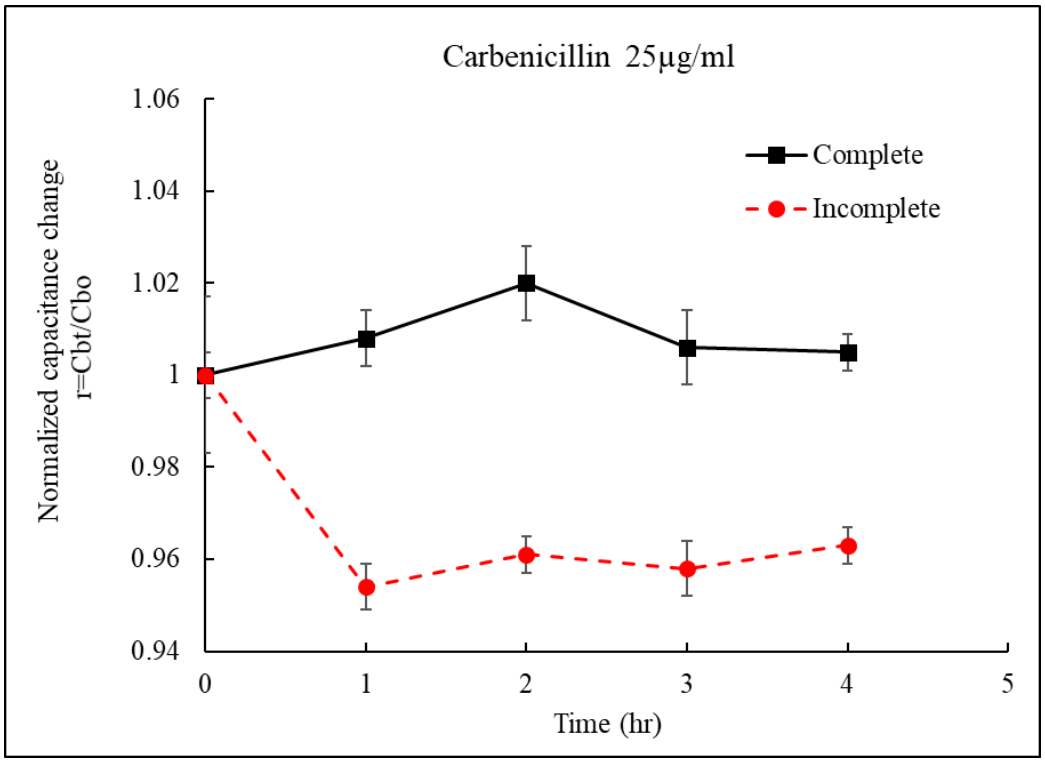

Figure 3.6 Incomplete decontamination causes false-positive results. Bulk capacitances decrease duce to the viable non-Mtb bacterial cells are present in the post decontamination process (*Mtb* is ~5x10^5 CFU/ml and n=5 at each data point).

Thus, we have reason to believe that with a disposable microfluidic cassette that has multiple channels (one loaded with carbenicillin, and perhaps 3 others loaded with high concentrations of cidal drugs like Amikacin, delaminid, and bedaquline, or their combinations), and a fixed unit card reader that can incubate the cards, perform electrical readings and provide a user interface, our technique can emerge as a low cost, a rugged system capable of providing same day results (detecting presence of live *M. tuberculosis* cells in sputum down to < 100 CFU/ml) at the point of need (regional hospitals and medical clinics.

3.5 Future work

As partly addressed in the discussion above, a number of questions remain unanswered by the current work. These include : (1) Will the method work for wild-type TB cells lodged in real human sputum? (2) If yes, how low can we get the limit of detection to?, and (3) Will the method continue to be effective even if the strains present are clinically resistant to the antibiotic(s) used? Even after answering these questions, we will have to establish whether the product foreseen (as described earlier) can be developed in a manner that is economically feasible – and hence make this method widely adopted?

To answer the question (1) above, the experiments need to be repeated with real-world sputum isolated from TB patients. An alternative would be to take real-world sputum from non-TB patients and spike it with TB strains isolated from clinical samples. Following the latter route may be more feasible since one could seed a multitude of strains with varying degrees of virulence and resistance to antibiotics (a range that would be very difficult to replicate with real world

samples) and also specify the load (CFUs) in the sample. This would also help us to address questions 2 and 3, above.

One can also explore other modifications to improve the technique (lower its limit of detection, turnaround time, and need for infrastructure such as centrifuges). For instance, functionalized magnetic nanoparticles can be used to concentrate the *Mtb* post-decontamination. This will not only replace the centrifugation process (thus facilitating this method's applications in low resources areas), but could also serve to reduce turnaround time (since it can be done faster than centrifugation) and further reduce the limit of detection (by concentrating all the cells from the sputum sample into a small volume).

Technology development to enable the proposed process to be widely adopted requires cost-effective manufacturing of a microfluidic cassette with multiple channels (perhaps 4) with carbenicillin (decontamination quality control) in one channel, and high doses of cidal antibiotics (individually or in combination) in others. It also requires the cost-effective implementation of m-EIS (which is currently done with an expensive impedance analyzer) by building dedicated low-cost card-readers and data analyzers. To implement the sample-prep steps, it might also be beneficial to produce a reagent kit (along with well-specified instructions) to go along with the cassette and the hardware. And finally, this set of products need to be tested in the field.

CHAPTER 4
A RAPID SENSING PLATFORM TO EARLY DETECTION OF MICROBIAL CONTAMINATION IN BIOETHANOL FERMENTATION PROCESSES

4.1 Introduction

Attaining energy independence and enabling a truly sustainable chemical industry will only be possible with efficient and cost-effective biorefineries able to convert renewable feedstocks in the United States[58]. However, the development of biorefineries has been hampered by poor economics in the last decade, which cannot compete with gasoline. Bioethanol is arguably the most advanced alternate energy source, with over 15 billion gallons of fuel ethanol produced each year in the US using yeast fermentation[59]. Due to the operation scale, fuel ethanol is not made under aseptic conditions, and microbial contamination is common[58, 60]. Among these contaminating microorganisms, the lactic acid bacteria (LAB) are widely considered to be the most problematic[61, 62]. LAB contamination reduces sugar available for ethanol production and depletes micronutrients required for optimal growth of yeast, thus causing not only lowered yields [63], but also instances of "stuck" fermentation[64, 65], where the fermentation has stopped before all the available sugar is "used up". A contamination event not only harms the current (contaminated) batch, but also necessitates costly shutdowns of facilities for cleaning. Traditional approaches to mitigate LAB contamination involve acid cleanse of the process equipment and/or the use of antibiotics such as penicillin and, more recently, virginiamycin[66]. These approaches are not only expensive, they also lead to the emergence of antibiotic resistance LAB and pose serious

environmental hazards. Therefore, there is a great demand to take preventive measures to minimize the incidence of contamination.

The problem of contamination becomes most severe if the inoculum stream itself becomes contaminated (since this provides maximum time and maximum nutrients for the bacteria to compete with the yeast). Studies [67] indicate that introducing inocula with ~10^5 CFU/ml of Lactic Acid Bacteria (LAB) could reduce the yield of ethanol by ~8%. Others have estimated the reduction of yield to be in the 20%-30% range [68]. In addition, the presence of LAB in the inoculum is also believed to be responsible for the “stuck” fermentations observed[69], which as indicated earlier, require costly shut-downs.

The process of preparing the inoculum for these large-scale fermenters is depicted in Figure 4.1. As shown, the inoculum train starts with the transfer of yeast cells from either a cryopreserved stock or dried yeast into ~1L shake flask containing growth medium (typically synthetic or defined) and ample aeration to generate biomass. After a dense culture is obtained, the culture is transferred into ~1000 Gallon aerated fermenters to produce the seed for large anaerobic fermenters. Prior to transferring the output of the 1,000 Gallon fermenters into the production tank for use as inoculum, it is tested to check for the presence of Lactic Acid Bacteria (LAB). If these tests indicate the presence of LAB in any of these batches, then that particular one is discarded. The ones in which no LAB are detected may be pooled and fed as inoculum into the production tank, thus generating a larger inoculum pitch.

There exist multiple methods to detect the presence of LAB in the yeast inoculum, the most common of which are listed in Table 4.1, along with their key attributes such as the limit of detection, the time needed to perform these measurements, and approximate cost per sample.

Table 4.1 Methods available for the detection of Lactic Acid Bacteria (LAB)

Approach	Method	Limit of Detection	Time	Approximate Cost
HPLC	Indirect (lactic acid)	~0.2 g/L	2 hrs.	$45
LC-MS	Indirect (lactic acid)	~ 5 ng/L	2 hrs.	$150
Enzyme Assay Kit	Indirect (lactic acid)	~ 0.2 mg/L	3 hrs.	$175
PCR/DNA sequencing	Direct (DNA)	~1,000 CFU/mL	4 hrs.	$300

As can be seen, molecular methods based on Polymerase Chain Reaction/DNA sequencing have the lowest limit of detection, but are very expensive and require trained personnel. The other methods are indirect: in the sense that they do not detect LAB cells, but rather the product of their metabolism: viz. lactic acid. Of these, High-Performance Liquid Chromatography (HPLC) is the technique most commonly used in the bioethanol industry to detect the LAB contamination because of it is quick and low-cost. However, it has a relatively high detection limit (of ~0.2 g/ml[70]). Mathematical models [67] indicate that, in order to achieve this level of lactic acid in the broth, $>10^7$ CFU/ml of lactic acid bacteria (LAB) must be present. This implies that there are probably a number of cases where LAB are present in the inoculum, but because their concentration is lower than $\sim10^7$ CFU/ml, they remain undetected. When such inoculums are used to seed the production reactor, it results in lower ethanol production and/or stuck fermentations.

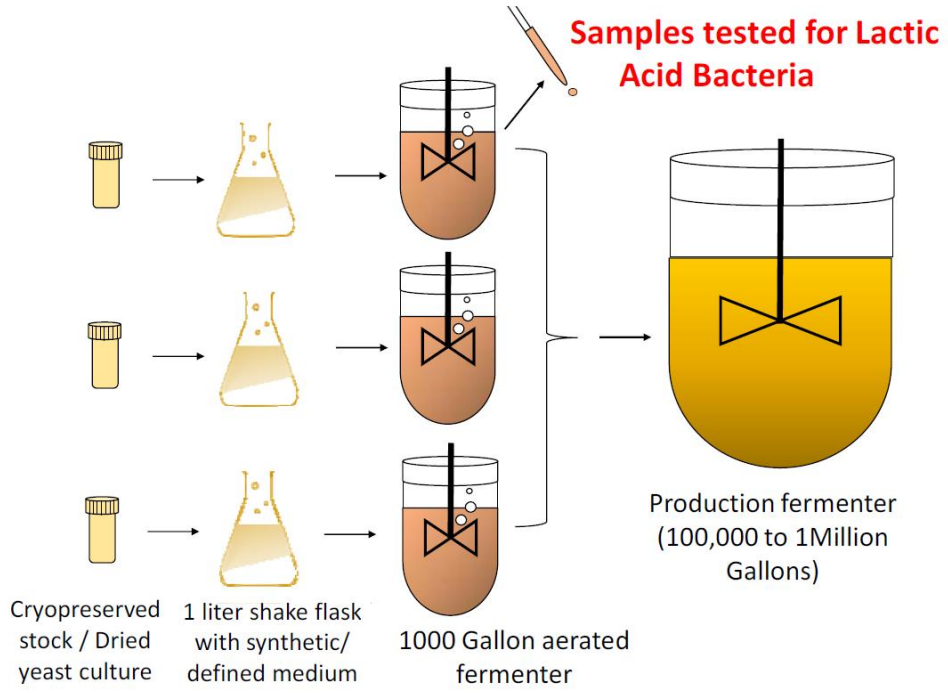

Figure 4.1 For bioethanol fermentation, the inoculum train starts with yeast cells' transfer from either a cryopreserved stock or dried yeast into ~1L shake flask containing growth medium and ample aeration to generate biomass. After a dense culture is obtained, the culture is transferred into ~1,000 Gallon aerated fermenters to produce the seed for large anaerobic fermenters. Before moving the output of the 1,000 Gallon fermenters into the production tank for use as inoculum, it is tested to check for the presence of Lactic Acid Bacteria.

Currently, no sensor can directly detect viable LAB cell in low quantities with rapid turnaround time. Through this study, we aim to develop a sensor platform to fill this void. The sensor platform being developed in this proposal promises to play a pivotal role in detecting the contamination early to allow the opportunity to take corrective action. We proposed to use microchannel electrochemical impedance spectroscopy (m-EIS) [5]) to directly detect the presence of LAB in the fermentation broth. The m-EIS method relies on the fact that in the presence of high-frequency AC electric fields, the membranes of cells become polarized and store charge, thereby acting like electrical capacitors [6].

These capacitances at the individual cells contribute to the suspension's overall "bulk capacitance" (net charge stored in the interior). The amount of charge stored by a live bacterium is about 100x of an equal volume of aqueous solution[7]. Thus, even at low concentrations (volume fractions), bacteria in a suspension contribute significantly to the latter's bulk capacitance. Our previous test results show that m-EIS can detect bacterial growth with very low detection limits of is ~1000 CFU/ml in blood[57], food samples[56], and bacterial growth broths[3]. By the concept of "detection by death"[51, 55], m-EIS can detect bacteria with a short of detection time In this work, we will present a novel method for detecting LAB at concentrations as low as 10^3-10^4 CFU/ml.

4.2. Materials and methods

4.2.1 Method overview

Figure 4.2 shows a schematic of our experimental protocol of LAB detection by m-EIS biosensor. First, LAB is isolated from fermentation broth using filters. Then, beta-lactam antibiotics are added at a high dose to kill LAB[71]. Finally, the filtrated broth with an antibiotic is introduced into a microfluidic channel, monitored electrically for the next 2-4 hours using m-EIS. The m-EIS measure the "bulk capacitance (C_b)" of the cell suspension in the microfluidic channel. Since the bulk capacitance (C_b) has a relationship with the number of live LAB cells in the testing channel, if the bulk capacitance (C_b) decreases during the testing, one can tell that LAB is present in the fermentation broth.

.

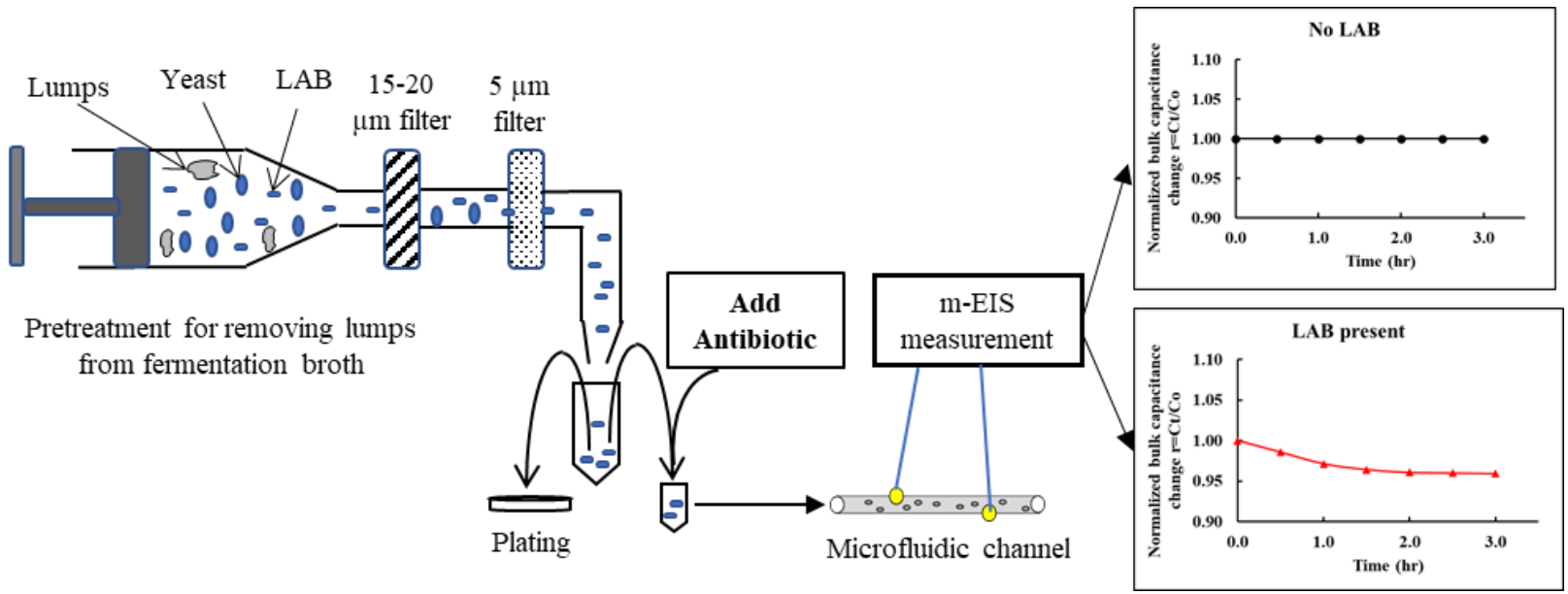

Figure 4.2 Schematic of the proposed approach to rapidly detect low numbers of Lactic Acid Bacteria (LAB) contamination in the bioethanol fermentation. This proposed method includes a LAB separation process and m-EIS measurement.

4.2.2 LAB and Yeast strains

In this study, three strains of lactic acid bacteria (LAB), *Lactobacillus acidophilus* (ATCC 43121), *Lactobacillus fermentum* (ATCC 9338), and *Lactobacillus casei* (ATCC 393) were used as representatives of bacterial contamination in the bioethanol fermentation. All these LAB strains were purchased from ATCC and were subcultured in MRS broth in our lab. Ethanol Red® was chosen as a representative yeast used in bioethanol production. We obtain this yeast stain from a local bioethanol plant and subcultured in YPD broth in our lab.

4.2.3 Fermentation broth preparation

We prepared the fermentation broth to closely resemble broth often used for aerated fermentation of yeast cells. Briefly, we prepared 100ml broth by adding 16.4 ml of corn syrup (to prepare it by adding11g sugar in 30ml of syrup) to 83.6 ml DI water. Then, add the supplements of 0.002 g/L of KH_2PO_4, 0.002 g of $(NH4)_2SO_4$, 0.001 g of $MgSO_4$, 0.015g of yeast extract, 0.015 g of peptones, and 0.0015 g of urea. The contents were mixed well and then filtrated-sterilized by passing the solution through a 0.45 µm syringe filter. The sterile broth was stored in a 4°C refrigerator prior to use.

Since this study is to detect lower concentrations of LAB, samples are supposed to be taken from the aerated fermenters, LAB and yeast will grow in an aerobic environment. We added 50mL of fermentation broth to a sterile 250 mL flask with a magnetic stir bar and sponge plug cover. Aliquots are kept on a magnetic platform to achieve uniform mixing and adequate aeration.

4.2.4 LAB separation by filtration

Although yeast cells cannot be killed by beta-lactam antibiotics (ampicillin) and not contribute to the bulk capacitance decreasing in bulk capacitance of the testing channel. Given that 2-4 hours of testing time, yeast cell division (proliferation) could lead to bulk capacitance increase, which can "neutralize" LAB's cell death. We separate the LAB from yeast before the m-EIS test.

Filtration is a simple physical method to separate and collect yeast or bacteria from the fermentation broth. Researchers have previously shown that serial filtration with membrane filters can separate yeast cells from bacteria efficiently for beer and wine fermentation [72]. Inversely, similar methods will be used to separate yeast from fermentation broth and retain these LAB contaminants in the filtered broth for m-EIS measurement.

Based on the cell size measurement under a compound microscope, yeast cells are spherical with a size of 7-15 µm. In comparison, the LAB are rod-shaped with a size of 0.5-1.2 µm by 1.0-5.0 µm [14]. A 5 micrometers syringe filter (Whatman) will be used to retain all the yeast cells and let the LAB cells pass.

We use the commercially available syringe membrane filter to filtrated about 1.5 ml of fermentation broth to collect about 500 µL of filtrated broth. There are about 1 ml of broth will be trapped in the void space of the filter itself. Briefly, we followed the steps: a) prepare yeast culture in the fermentation broth, then incubate at 32˚C for two days to achieve concentrations of ~10^9 CFU/mL. b) spike LAB into the yeast culture for ~10^7, ~10^5, and ~10^3 CFU/mL, respectively, and c) homogenize it, and pass through the filter. d) collect filtrated broth after 5

μm filters. e) Finally, plate filtrated broth on the YPD (with ampicillin to inhibit LAB's growth, 16mg/L) and MRS (with cycloheximide to suppress yeast's growth, 32mg/L) to evaluate the LAB collection efficacy.

4.2.5 Microfluidic channel and m-EIS measurement

This microchannel consists of a 3D printed top PMMA part and a glass slide base assembled by a biocompatible epoxy (Epo-Tek 301TM, USA). It has electrodes asymmetrically placed 10mm apart, as shown in figure 4.3(b). It thus allows the user to assay a fluid volume of ~10μL (~10mm length x 1mm width x 1mm height) between the two electrodes in the microchannel. The two electrodes will be connected to the high precision impedance analyzer (Agilent/Keysight 4294A) to measure the impedance (resistance (R) and reactance (X)) of the channel between the electrodes. The m-EIS measurement was then performed every 30 minutes for 2-4 hours by using an AC signal of 500 mV amplitude in the range of 1k Hz to 100M Hz was applied to the electrodes.

After the fermentation broth was filtrated, we use a concentration of 16 μg/L ampicillin to kill LAB. According to our test results of the plating count method, a dose of 16 μg/L is high enough to kill the three strains of LAB in a short time. A small aliquot of 20 μL of the testing solution was injected into the microfluidic channel. The measurement was taken every 30 minutes for about 2-4 hours.

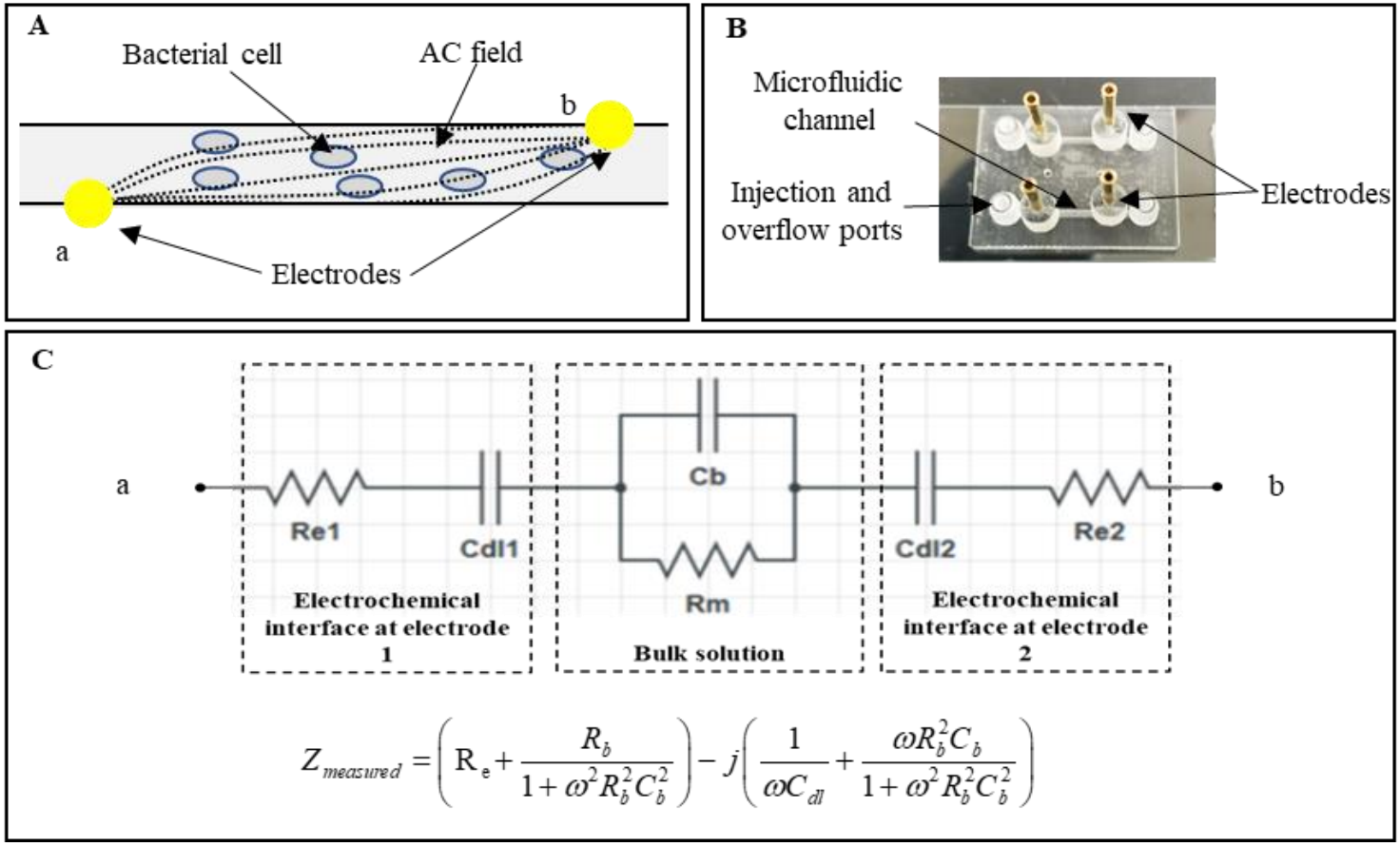

$$Z_{measured} = \left(R_e + \frac{R_b}{1+\omega^2 R_b^2 C_b^2} \right) - j\left(\frac{1}{\omega C_{dl}} + \frac{\omega R_b^2 C_b}{1+\omega^2 R_b^2 C_b^2} \right)$$

Figure 4.3 schematic of m-EIS and electrochemical circuit model. (a) bacterial cells are under AC filed in a microfluidic channel. (b) a 3D printed microfluidic channel. (c) the equivalent circuit for microfluidic channels and impedance equation, where C_b denotes the bulk capacitance of the microchannel; R_e denotes resistances of electrodes; C_{dl} denotes double layers capacitance, and Rm denotes bulk solution resistance.

4.2.6 Analysis of m-EIS data

A modeling software ZView® (Scribner Associates, USA) was used to extract these parameters of the equivalent circuit for this microfluidic channel with bacteria cell suspension[3]. The bulk capacitance (C_b) is related to the viable LAB cell number in the microfluidic channels. As shown in figure 3.3(c) in chapter 3, the bulk capacitance values will be plotted in a bulk capacitance (F) vs. time (hr). Then, normalized bulk capacitance (C_{bt}/C_{bo}) will be plotted to check the bulk capacitance change.

Mann-Whitney U test will be used to tell that there is a significant bulk capacitance change at every time measurement (t>0hr) comparing to the baseline (t=0hr). If these data points (t> 0hrs) significantly lower than the baseline (t=0 hr), one can tell that LAB is present in the fermentation broth sample. The earliest points that significantly lower than baseline in time will be referred to as the detection times.

4.3. Results and discussion

The filtration test results show that a 5 μm pore size can retain all yeast cells and let LAB cells pass through (see the detail in appendix). As shown in figure 4.5 and table A2-1, A2-2, and A2-3, the LAB has about one order reduction in concentration on average for three different spiked concentrations tested in the yeast fermentation broth. There are sufficient LAB cells in the filtrate broth for the following m-EIS measurements, even with the single order reductions. m-EIS requires as low as $5x10^3$ CFU/mL cells to perform the LAB contamination test. Our m-EIS are ~3 log orders more sensitive than the current HPLC method (~0.2g/L LOD of lactic acid, equivalent to ~10^7 CFU/mL of LAB).

This one order reduction of LAB is due to the filter cake encountered in the filtration process[73]. We used a membrane filter to separate LAB from yeast is dead-end microfiltration. In the aerated fermenter, yeast cell concentration is as high as 10^9 CFU/mL. During the filtration, yeast cells will sediment on the surface to form the cake. In the real application, corn mash in the aerated fermenters will make the situation worse, leading to fewer LAB cells being collected after filtration. As shown in figure 4.2, a pretreatment filter with 15-20 micrometers will be used to mitigate the filter cake on the 5-micrometer filter by removing lumps (corn mash, slurry, etc.) and some yeast cells in the fermentation broth.

Except for the filtration method, nanoparticles have been used to isolate bacteria of interest in different complexes[74-76]. The collection efficiency nanoparticles have to be well elevated given that complicated environment in corn mash fermentation broth. However, we can use nanoparticles to concentrate the LAB cells after the filtration process. In that case, it can help us to improve the detection sensitivity and lower the detection limit for the following m-EIS measurement.

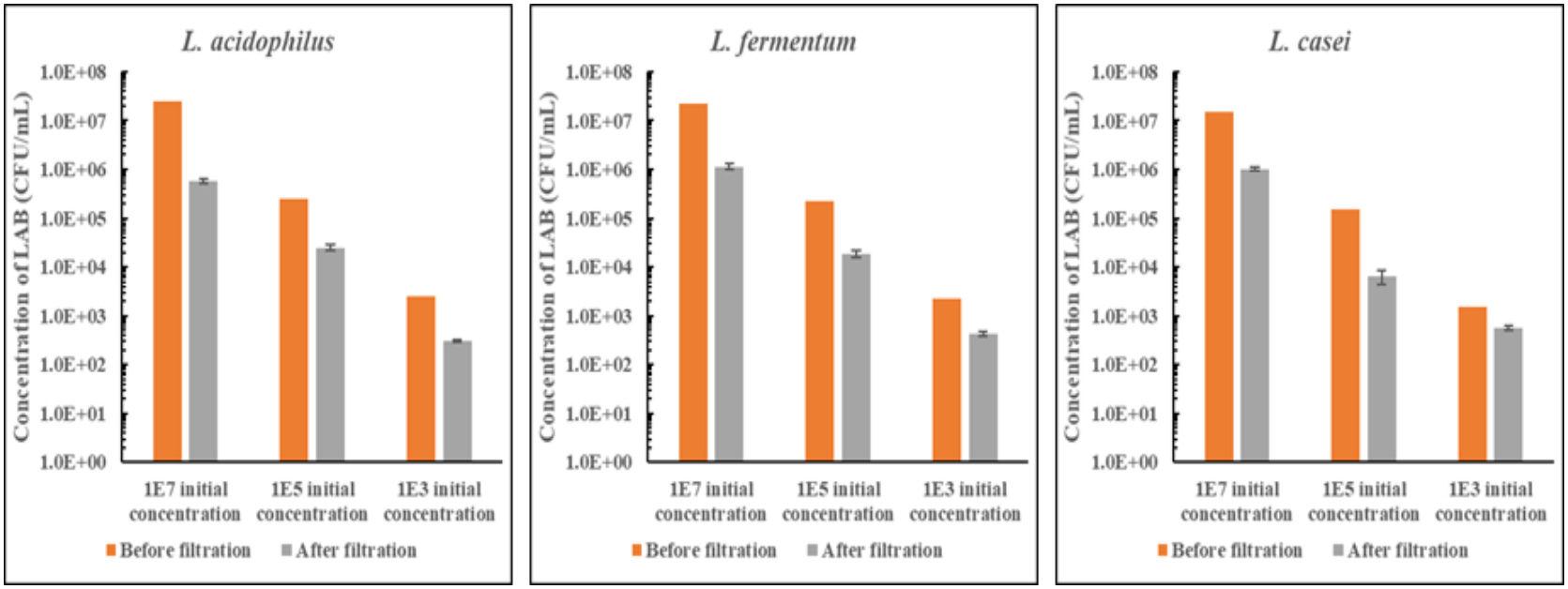

Figure 4.5 Collection efficiency for LAB from the fermentation broth. The LAB has about one order reduction in all testing concentrations (10^3, 10^5, and 10^7CFU/ml) on average.

As shown in Figure 5a,5b, and 5c, in the presence of a high dose of antibiotic of ampicillin, all 3 strains of LAB show decreasing trends of bulk capacitance (C_b), except for the controls (no LAB present). This decrease of bulk capacitance (C_b) is directly correlated with the death of LAB cells in the suspension. The death of LAB was also confirmed with the initial and end of the experiment plating of sample onto MRS agar plates (data not shown). Mann-Whitney U test indicates that all strains of LAB with various concentrations have a significant decrease of bulk capacitance (C_b) at/after 1 hour.

In all three strains of LAB, the bulk capacitance (C_b) drop was observed in 30 minutes to an hour, indicating that the assay time to determine the presence of low LAB concentrations in fermentation broths can be less than 2 hours. Thus, the system will have a fast turnaround time on sample testing. Our method can detect a low concentration of ~5000 CFU/ml, which is about 3 orders lower than the current HPLC method (~0.2 g/L LOD of lactic acid, equivalent to ~10^7 CFU/mL of LAB).

As shown in the filtration test results, there is about one order reduction for LAB, which means the detection limit will be about 10^5 CFU/mL in real applications of m-EIS method. To overcome the reduction from filtration, one can employ bacteria cell concentration techniques to elevate the LAB concentration that before performing the m-EIS measurement. Centrifugation or retaining the LAB on a 0.45-micrometer filter then resuspended in a smaller volume could be a simple way to accomplish that. Our previous research has recently shown that magnetic nanoparticles can isolate the bacteria of interest from samples but do

not contribute to the bulk capacitance change during the m-EIS measurement for the cell suspension[55].

Due to the antibiotic resistance LAB stains merging, drug susceptibility tests (AST) become necessary for the antibiotic treatment for LAB contamination. In addition to the LAB detection function, m-EIS can provide a rapid AST for proper antibiotic treatment. On the other hand, the merging of resistance LAB stains can be a challenge for the concept of "detection by death". A higher efficiency way to fast kill LAB has to be explored, such as using a cocktail of antibiotics strategy to combat bacterial resistance [21] or integrating a UV radiation device in the m-EIS platform to kill bacteria.

As we mentioned above, (incorrect or overdoes) antibiotic treatments for LAB contamination have posed environmental issues and antibiotic resistance LAB stains merging. The way to cut off the evolution of antibiotic resistance in the bioethanol fermentation is that when the treatment is necessary, use as little as possible of antibiotic. With the low detection limit and short detection time to LAB with the m-EIS method, it could make that possible.

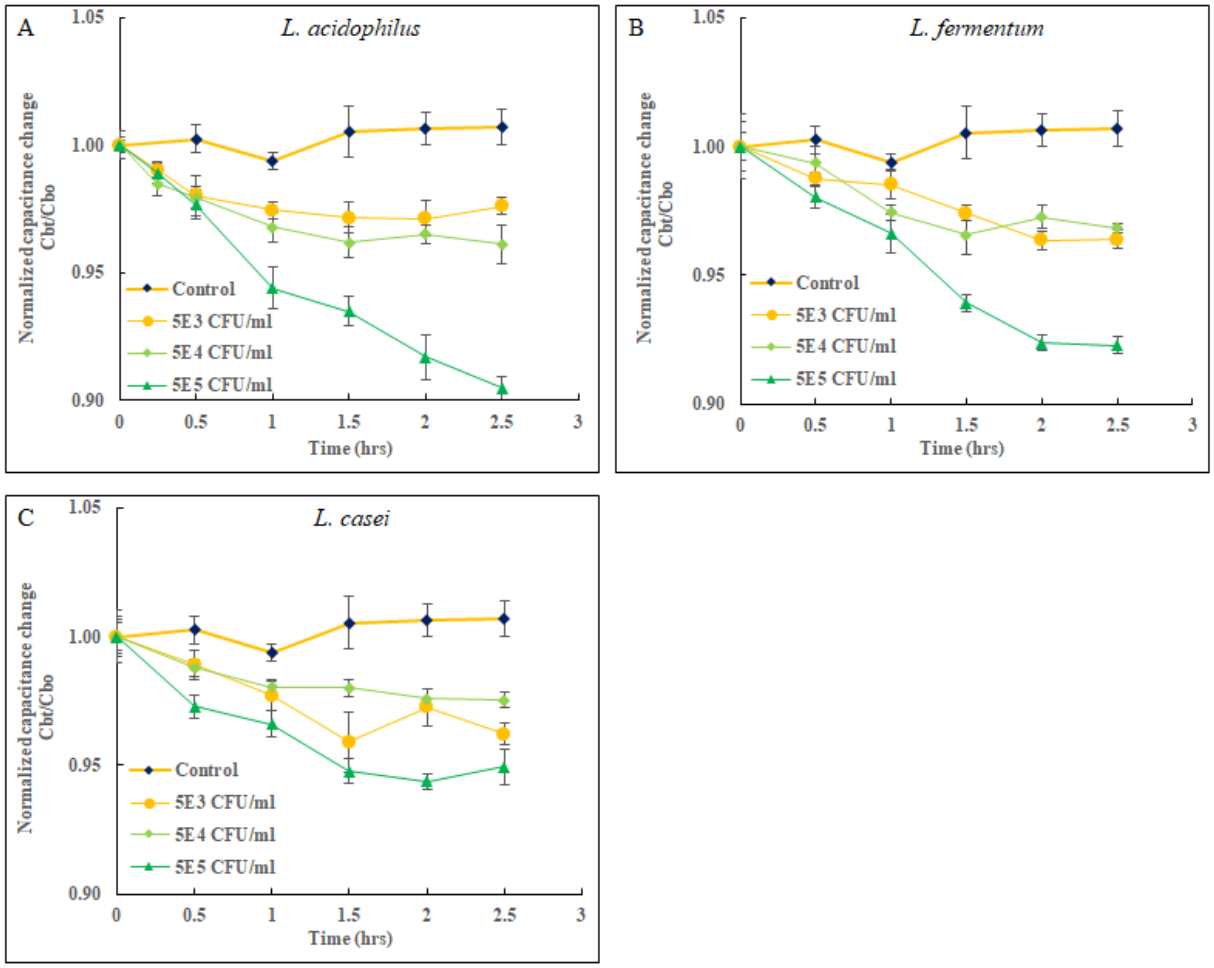

Figure 4.6 Changes in bulk capacitance (Cb) (scaled to time t=0 value) as a result of exposure to antibiotic (typically, n=5 at each point in time)

4.4. Future Work

Thus, we have demonstrated the m-EIS can detect LAB contamination in 2 hours with a detection limit of ~ 5 x 10^4 CFU/ml in the fermentation broth. While this is about 1000 times lower than the current limit of detection using HPLC, we believe there is scope for further improvement.

Currently, the filtration process results in a decrease in the concentration of LAB present by approximately 1-$\log_{10}$. A well-designed pretreatment system which can isolate the LAB from the fermentation broth without this loss will immediately improve the process ten-fold. We have currently used off-the-shelf general-purpose filters (with a large surface area and residual volume between the two filters) to remove the yeast. A filtration system designed specifically for this application will be able to isolate the LAB more efficiently. Alternatives such as Magnetic Nanoparticles (MNPs) can also be explored to achieve more effective isolation.

The method could be further extended to monitor ongoing fermentations in near-real time for the presence of contaminating bacteria (specifically LAB). Lactic Acid Bacteria are contaminants not only for ethanol production by yeasts, but also for other yeast fermentations such as those for beer and wine. Aliquots from large fermentation reactors (that often run for days) could be analyzed for the presence of LAB, results be made available within 2-3 hours, enabling corrective action be taken to adjust the process (or at least terminate the process early to minimize losses).

Currently, antibiotics are sometimes introduced into fermentations are latter stages to kill contaminants that have been discovered. Since our m-EIS method

has also been used to establish minimum inhibitory concentrations (MICs) of microorganisms in a clinical setting, one could foresee doing so for contaminants detected in fermentations as well. Knowing the MICs would enable optimum use of antibiotics, which will serve to reduce process costs and make the process more environmentally friendly (reduce widespread use of organisms in the environment, which fosters antibiotic resistance).

Although the contamination that we focused on in this study is due to LAB, other microorganisms such as wild yeast[77-79], also affect the productivity of these bioethanol fermentations. So, by applying the “detection by death” concept, our m-EIS could detect contaminant yeast in the fermentation with the right selection of the anti-yeast compounds (killing agents for contaminant yeast detection).

CHAPTER 5
USING ELECTROCHEMICAL IMPEDANCE SPECTROSCOPY TO DETECT BIOFILM FORMATION.

5.1 Introduction

Biofilms are a complex group of microbial cells enclosed in an exopolysaccharide matrix present on a surface, common to find on the surface of medical devices or implants. Due to its resistance to antibiotic treatment[80, 81] and a low-grade immune response[82], biofilm formation and growth on the surface of medical devices or implants that associated infections cause a severe problem to the patients' health and adversely affect the function of the medical devices or implants[83-85]. According to the Centers for Disease Control and Prevention (CDC), millions of people in the U.S. suffer microbial infections involved with biofilm. Biofilm phenotype bacteria cause 65 to 80 percent of all human infectious diseases [86].

There are two ways to treat or inhibit biofilm formation to minimize health problems, anti-biofilm drug or antibacterial substances discovery and development[87], and antibiofilm coating layer[88], or surfaced with antibiofilm nanostructures[89]. A high throughput method is an urgent need to be developed to evaluate the effectiveness of a new drug or surface modification.

More than two decades ago, researchers relied on scanning electron microscopy (SEM) or standard microbiologic culture techniques for biofilm characterization[90]. Recently, the confocal laser scanning microscope has been used to characterize biofilm ultrastructure and investigate bacterial cell adhesion and biofilm formation mechanisms. However, these image-based methods have a disadvantage for the new antibiofilm drug discovery and antibiofilm materials

screening. They are invasive, labor-intensive, expensive, and not real-time biofilm study methods[91].

Since biofilm is forming and growing on the substrate's surface, such as metals and metal alloy implants, looking for the surface characteristic change can directly monitor the biofilm formation. The impedance can provide the bacterial cells attached to the surface under an electrical field for the metal-based implant. Impedance-based sensors have the potential to be developed as a non-invasive and real-time monitoring method to study biofilms. Giaever and Keese have explored using electrodes under an electric field to monitor cell behavior[34]. Ramasamy et al. used the impedance method to study biofilm formation on electrodes of microbial fuel cells[92]. But, most of these impedance-based sensors are not sensitive and accurate detection methods to study biofilm[93, 94]. They measured the impedance change at a single frequency or can't eliminate the death cells' contribution to the impedance changes.

Here, we propose to use electrochemical impedance spectroscopy to monitor biofilm formation. It can meet the requirements of a real-time, label-free, and low-cost EIS-base sensor platforms to detect biofilm formation and growth on the medical implants and/or to effectively and inexpensively screen new biomedical anti-biofilm materials.

5.2. materials and methods

5.2.1 method overview

Figure 5.1 shows a summary of the test protocol. As shown in the figure 5.1(a), biofilm will be grown in a homemade EIS adapted cell culture plate for the real-time measurement, where, the two stainless steel electrodes are connected

to the high precision impedance analyzer (4294A, Agilent, USA) through a test fixture (16047E, Keysight, USA) and the data will be collected by a computer. Figure 5.1(b) shows that an EIS adapted cell culture plate. Biofilm's formation and growth will be measured on the surface of the two electrodes. Figure 1c shows that the EIS measurement setup, the EIS adapted cell culture plate is incubated in a homemade incubator.

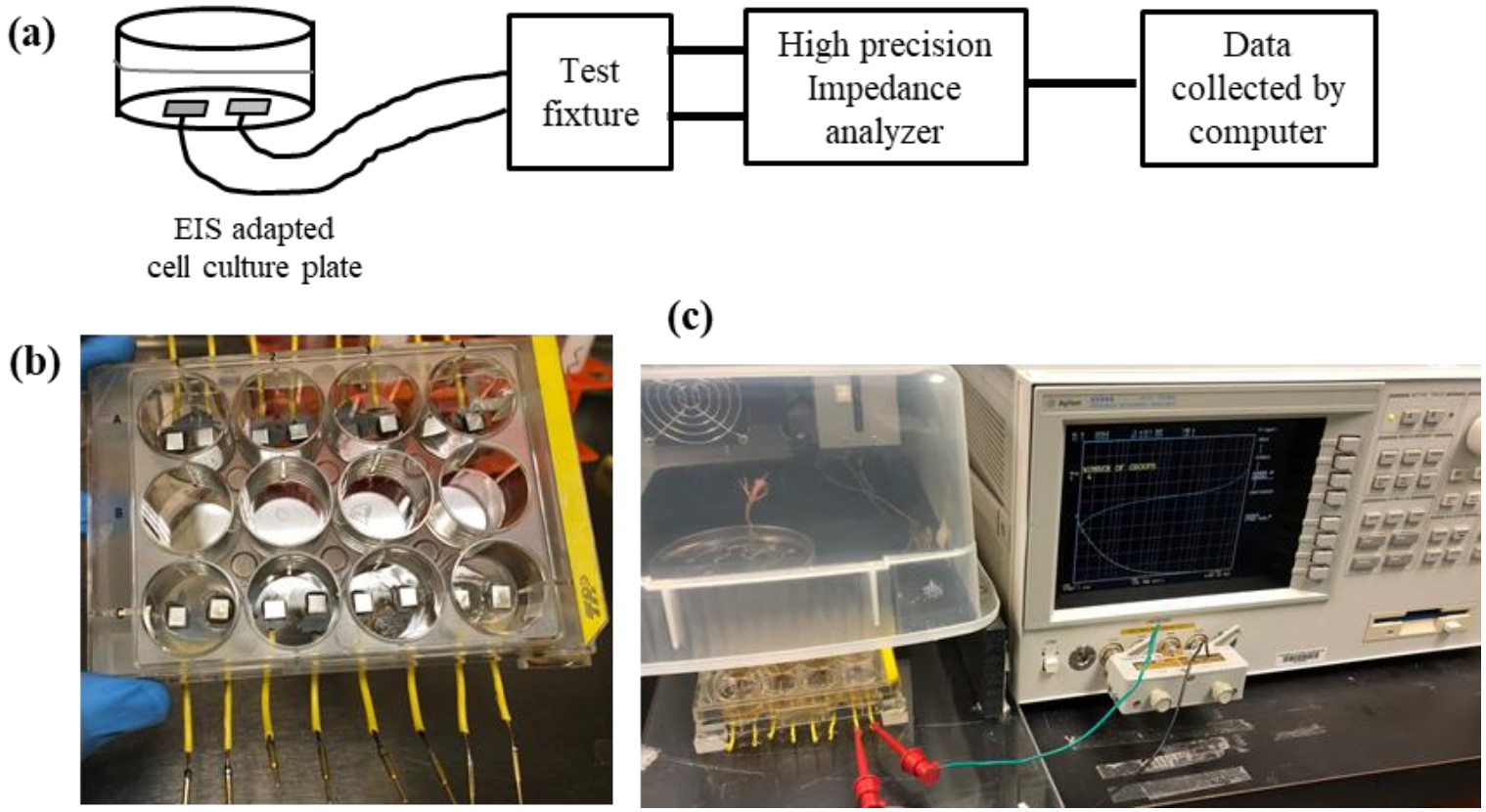

Figure 5.1 (a) Schematic of the method monitoring biofilm growth using electrochemical impedance spectroscopy. (b) an EIS adapted cell culture plate where two stainless steel electrodes are built at the wells' bottom. (c) EIS measurement setup, the EIS adapted cell culture plate is incubated in a homemade incubator.

5.2.2 fabrication of EIS adapted cell culture plate

316L stainless steel, which is widely used as implants as biomaterials[95], will be used as an implant material for biofilm formation and growth study. As shown in figure 5.1(b), an EIS adapted cell culture plate is a composite of one 12-well flat-bottom plate, two pieces of 0.5cmx0.5cm stainless steel sheet, and two 18 AWG solid copper wires. To fabricate it, one side of the stainless steel sheet was coarsened by a grinding point, and then an 18 AWG solid copper wire was soldered on it. At the bottom of the well, two small holes (an 18 AWG solid copper wire size) were drilled for the two conductive wires on the stainless steel sheet going through it. Then, biocompatible epoxy (EPO-TEK® 310M-1, Epoxy Technology, USA) was used to seal the gap between the holes and wire and keep water (broth) proof.

Before using the EIS adapted cell culture plate, it was disinfected by 75% alcohol and then rinsed 7 times by DI water. After air-dried in a biosafety level two cabinet, it will be kept in a sterile condition under the UV light (from the biosafety cabinet) for 30 minutes.

5.2.3 TMS plasma coating on stainless steel

As anti-biofilm coating material on the stainless steel sheets, trimethylsilane (TMS)[96] was used in this study. This plasma coating method was similar to the previous researchers[97]. Briefly, after one side of the stainless sheet was soldered with a piece of conductive wire, which was described in section 5.2.2, then, Stainless steel sheets with conductive wires were washed 7-8 times to remove the solder paste. Stainless steel sheets with wires were hung in the plasma coating chamber and then coated with TMS (Gelest Inc., USA) in a 50

millitorrs pressure following the oxygen plasma cleaning. TMS was excited by a DC power of 5 watts for a 15 seconds coating time in the chamber as shown in figure 5.2.

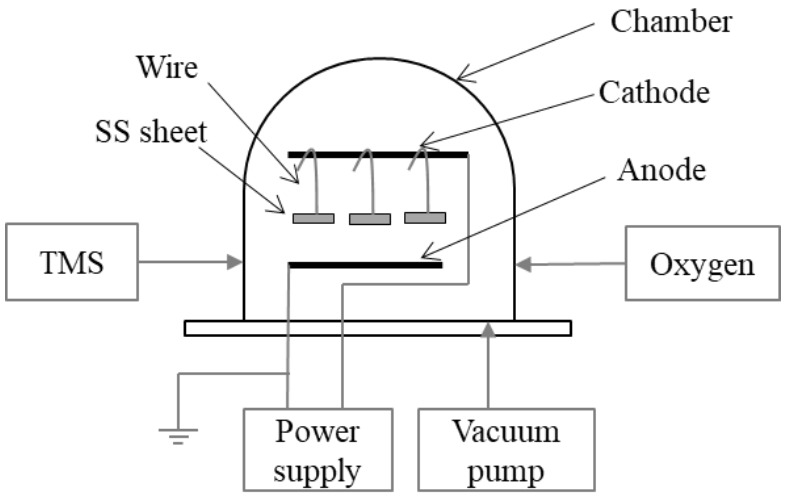

Figure 5.2 TMS plasma coating system. The SS sheets were clean by oxygen plasma and then coated with TMS in a 50 millitorrs pressure chamber.

5.2.4 bacterial strain and growth conditions

Staphylococcus aureus HT 20020073, also referred to as NRS234, was used in this study as a biofilm-forming strain. It was isolated in 2002 from the valve of a 3-year-old male with native valve endocarditis in France[98]. Previous studies[99, 100] have shown that it was capable of forming a biofilm, and it has been used to study biofilm formation on the surfaces of implants[97]. *Staphylococcus aureus* ATCC 29213 was used as a non-biofilm-forming strain.

Todd-Hewitt broth containing 0.2% yeast extract (THY) medium, 0.5% glucose was used to culture *S. aureus* at 37°C overnight. There, glucose was added to enhance biofilm formation[101]. Overnight cultured *S. aureus* was used

as the seed in a 12 cell culture plate or the EIS adapted cell culture plate, and each well had 2 ml of 1:200 diluted bacterial culture.

5.2.5 Scanning electron microscopy (SEM).

Biofilms of S. aureus formed on the stainless steel was visualized by scanning electron microscopy (SEM) as described by previous researchers[97]. Briefly, SS sheets were put in the bottom of the 12-well plate and the growth conditions were described in the section of 2.3, SS sheets were pulled out from the well plate to examine the biofilm formation from 0 to 12 hours. Then, the SS sheets with biofilm were processed by the flowing procedure. For each time, triplicates were performed.

The SS sheets with biofilms were gently washed four times with PBS to remove planktonic bacteria deposited on the surface and fixed with 2% glutaraldehyde–2% paraformaldehyde in 0.1 M cacodylate buffer (pH 7.4) for 2 h at 4°C. Then, the surfaces were washed three times with 0.1M cacodylate buffer (pH 7.4) and subsequently fixed with 0.1% osmium tetroxide for 1 h. After being washed in ultrapure distilled water, the biofilm samples were dehydrated by replacing the buffer with increasing concentrations of ethanol (20%, 50%, 70%, 90%, 95%, 100%, 100%, and 100%) for 15 min each. After critical-point drying and coating by platinum sputter, samples were examined using a Quanta 600F scanning electron microscope (FEI, USA).

5.2.6 Fluorescent staining of biofilm

Biofilms of S. aureus formed on the stainless steel was visualized by a fluorescence microscope. Biofilm formation has flowed the section of 5.2.5, SS

sheets were pulled out from the well plate to examine the biofilm formation from 0 to 12 hours.

Bacterial cells in the biofilm matrix were stained using a fluorescent nucleic acid stain kit (Invitrogen, USA) according to the manufacturer's protocols. Fluorescence-adherent bacteria were visualized with a fluorescence microscope (Olympus BX51, Japan).

5.2.7 EIS measurement

An AC signal of 500 mV amplitude in the range of 1000 Hz to 1M Hz was applied to the electrodes at the bottom of the EIS-adapted culture plate, where the biofilm formed on the electrodes' surface.

Here, the range of the frequencies was selected is at the center of the radio frequency range. At the interface between the electrolyte (broth) and the poorly conductive cell membrane, the relative dielectric permittivity of the cell is the β-dispersion[102]. The bacterial cells act as insulator spheres[27]. Other researchers have shown that under moderate frequencies, only a small current can flow under the edge of cells that grow on the surface of the electrodes[103]. So, the reaction between the bacterial cells that grow on the surface of electrodes and AC signals can be enhanced.

5.2.8 Equivalent circuit and EIS data analysis

As shown in figure 5.3, if no bacterial cells are growing on the electrode's surface, there will be an electrode/electrolyte interface in the Stern layer. Previous researchers treated that as an RC series circuit with the solution[34]. Here, we introduce the bulk capacitance[102] of the solution that is parallel with the solution's resistance. When the bacterial cells start to attach to the surface

and form a biofilm, the stern layer will be in a "hybrid" form. In these two situations, the interfacial capacitance will be analyzed to study the electrodes' biofilm formation. The equivalent circuit method will be used to analyze the value for each component. As shown in the figure 4.3c, in the equivalent circuit of a EIS testing well, Le presents inductor of electrode connection wire; R_e presents resistance of electrode connection wire and electrode; CPE-e presents constant phase of interfacial capacitance on electrodes; Rb presents resistance of ionic solution (media); and CPE-b presents a constant phase of bacterial cell in media (planktonic cell).

A modeling software ZView® (Scribner Associates, USA) was used to extract the equivalent circuit parameters. The interfacial capacitance (C_e) on the surface of electrodes is related to biofilm formation. Then, normalized interfacial capacitance (C_e), $r=(C-C_0)/C_0$, will be plotted to check the bulk capacitance change.

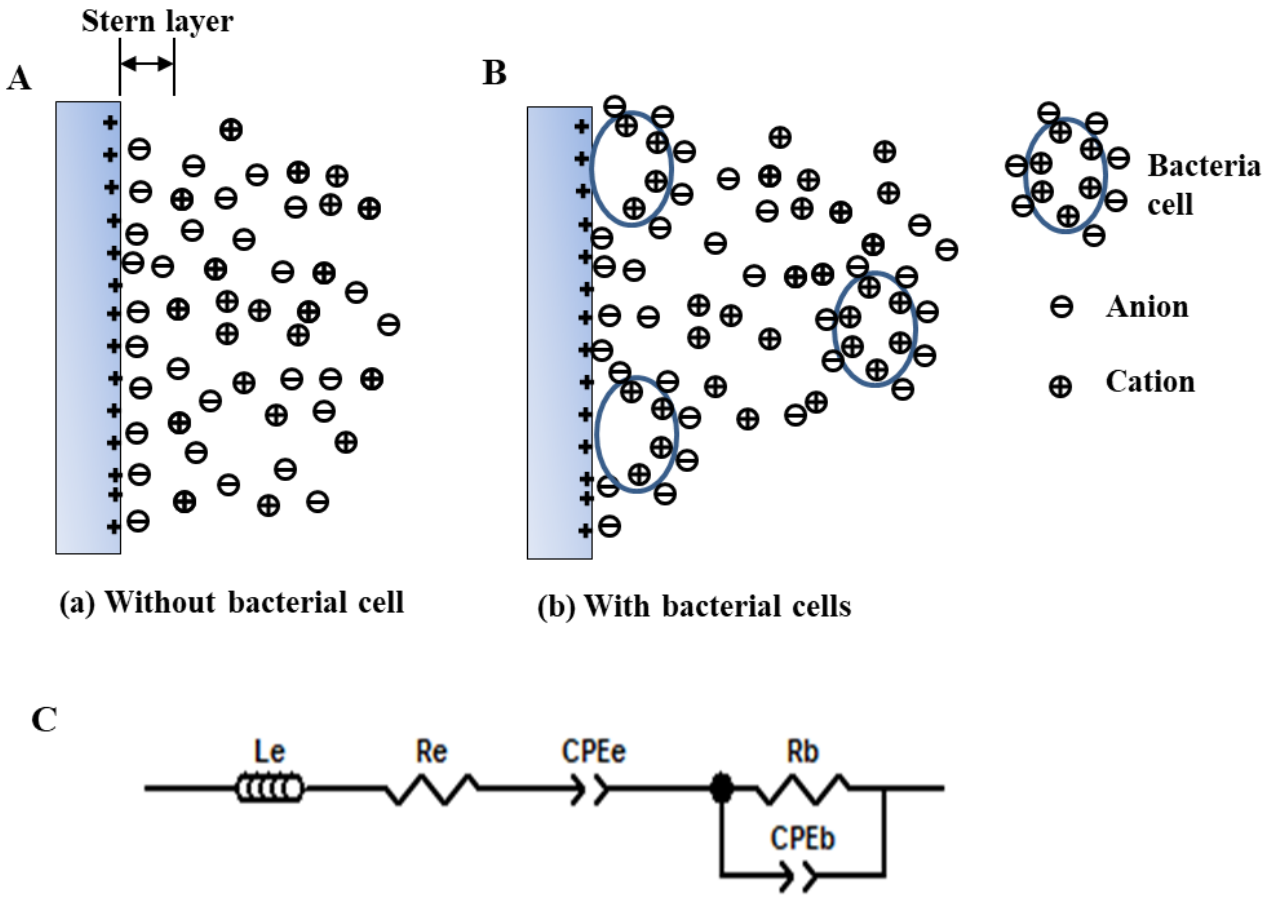

Figure 5.3 Interfacial capacitance and the equivalent circuits. a) interfacial capacitance of the Stern layer without bacterial cells b) interfacial capacitance with bacterial cells. c) equivalent circuit for the EIS testing well

5.3. Result and discussion

5.3.1 Impedance without biofilm

Figure 5.4 shows the values of the resistance of the uncoated SS sheet and coated SS sheet. The resistance is a function of frequency for both uncoated and coated. The phase angle trends to be small and positive as the higher frequency range, the measured capacitance will not be accurate and not useful for the study of the cells that grow on the surface, which due to the increase of the current through the cytoplasm of the bacterial cells[27].

Coated ss steel has higher resistance values comparing to the uncoated at the lower frequency range. According to the previous research results, the coating thickness on the SS sheet is about 20-30nm[97, 100], and the thickness of the oxidation layer is about 3-4 nm caused by plasma treatment[97, 100]. The resistance is dominated by the constriction resistance from the thin coating layer's pores on the ss electrode at the lower frequency range.

Using the equivalent circuit to fit the EIS impedance data, the interfacial capacitance of the uncoated SS electrode was estimated at 80μF/cm^2. Due to the coated SS electrode's porous property, after a 24-hour pre-soaking to let it get total wet, the interfacial capacitance is about 200μF/cm^2, higher than the uncoated electrodes. The porous surface has a larger area of the double capacitance layers.

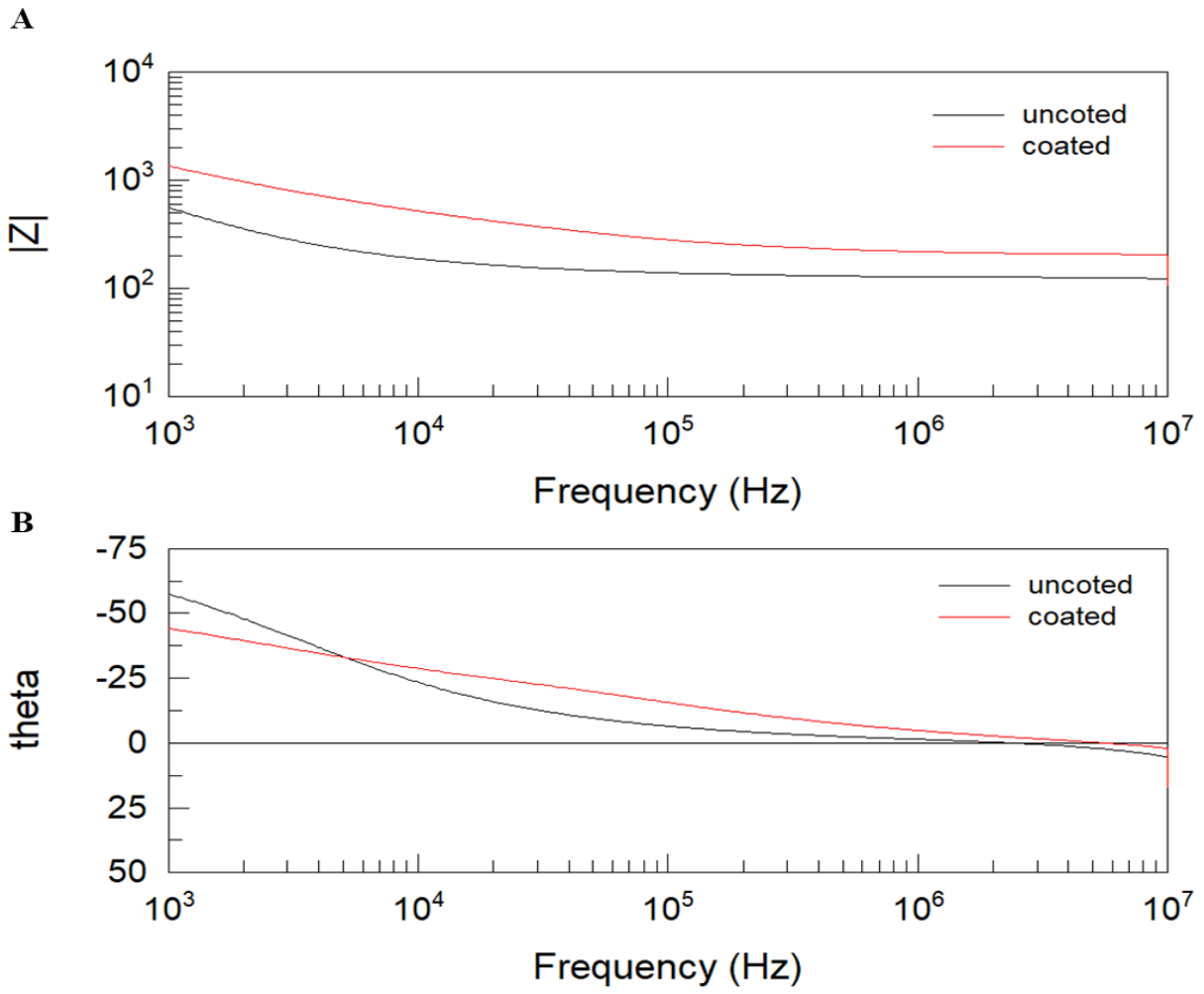

Figure 5.4 Impedance and phase angle for coated and uncoated SS electrodes. Due to a thin TMS coated layer, the coated SS electrodes have a higher impedance than the uncoated SS electrodes.

5.3.2 Impedance with bacterial growth in the EIS adapted well

As shown in figure 4.5(a), the RC circuit's total impedance on the uncoated SS electrodes decreased during the biofilm formation and development on the electrodes' surface. After fitting with the equivalent circuit, as shown in figure 5.3(c), the interfacial capacitance gets increased as biofilm forms on the electrode's surface. The normalized interfacial capacitance changes have been shown in figure 5.7.

We noticed that the interfacial capacitance slightly drops during the control test (media only) because the proteins and sugar components are attached to the SS electrode's surface, causing the dielectric constant to become smaller[104].

As a parallel experiment of biofilm formation investigation, Our SEM image (figure A4-1) showed that at the time of one hour, biofilm strain *S. aureus* planktonic cells were starting to attach to the SS sheet's surface. S. aureus cells attached to the surface were beginning to form biofilm matrixes with a multilayer of bacterial cells from the time of two hours. at the same time, the interfacial capacitance has an exponential upsurge with the fast biofilm-forming period. At the time of six hours, biofilm has developed to mature, and there were "mushroom" shape large matrixes of biofilm. The fluorescence image method (figure A3-2 and A3-3) was used to investigate biofilm's cell number. The results (figure A3-4) show a linear correlation between cell density and the values of interfacial capacitance from 0 to 4 hours.

Figure 4.7 shows that the RC circuit's total impedance on the electrodes slightly decreased during the non-biofilm strain *S. aureus* was growing in the EIS

adapted well. Its phase angle also decreased somewhat. After we fitted the impedance data by the equivalent circuit of figure 4.3c, we confirmed that, As shown in figure 5.7, the non-biofilm strain *S.aureus* has a slightly interfacial capacitance increased comparing to the control. We think that there could be two reasons that contributed to the capacitance increasing. One is the planktonic cells deposited on the electrode's surface cause the capacitance to increase. Our test results of the interfacial capacitance change study due to the planktonic bacteria deposited on the electrode surface show that planktonic cells deposited on the electrode's surface don't contribute to the capacitance to increase (figure A3-5). The other one is the non-biofilm strain *S. aureus* cells have attached to the electrode[105]. Although these bacterial cells can't form a biofilm, they have changed the electrodes' dielectric properties [103]. We also observed that the capacitance trend to flat after 2 hours because the non-biofilm stain bacteria cells attached to the electrodes cannot form biofilm matrixes where bacterial cells gather together.

Due to the bacterial metabolism, ionic concentrations, and ion species in the media will change. We have conducted the interfacial capacitance measurements with the aged. Our results show that the aged media have a slight impact on the capacitance values. But comparing to the capacitance from the biofilm is neglectable. In future research, the aged media consequence can be eliminated by changing the media every couple of hours or building a flow system with EIS testing.

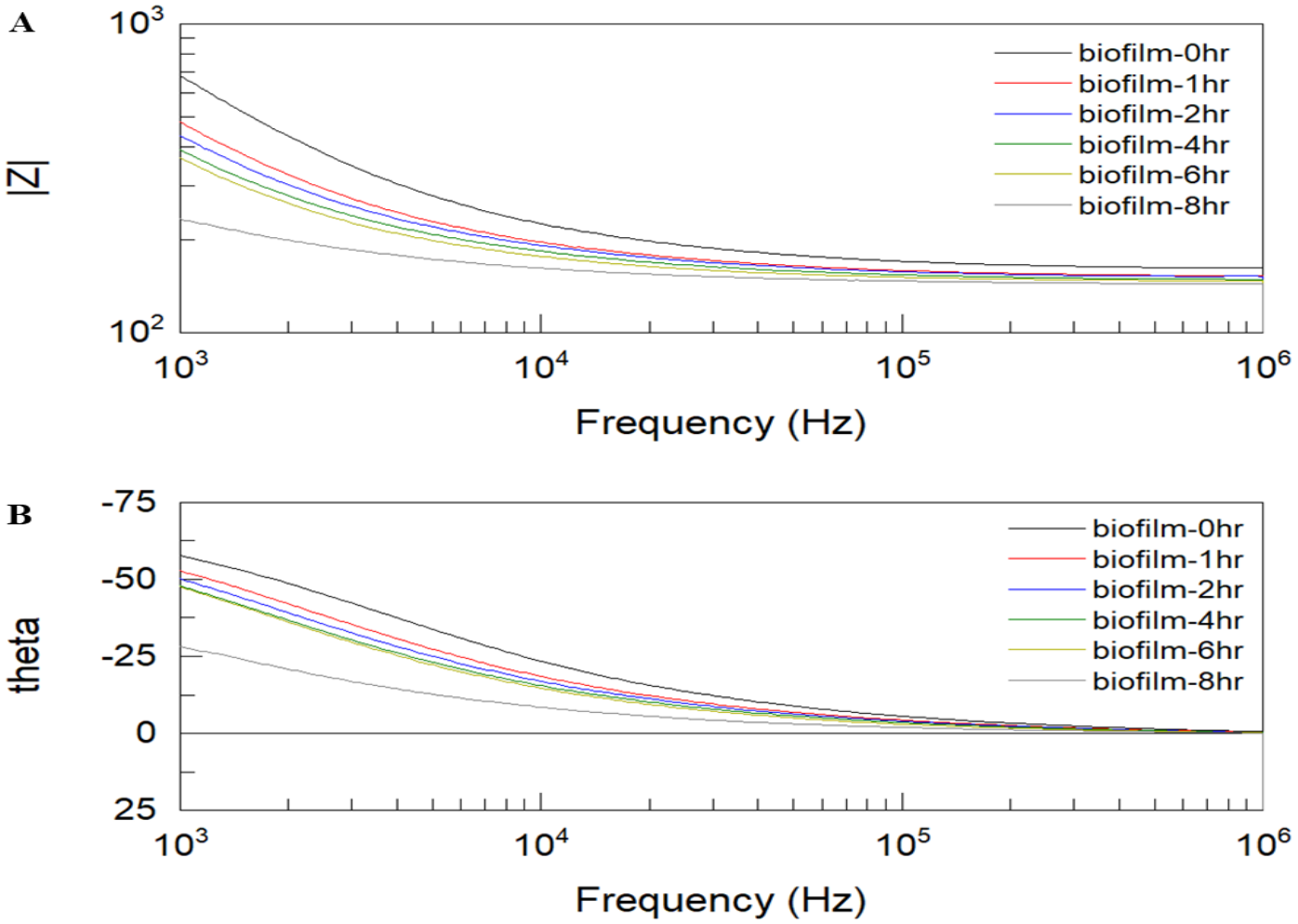

Figure 5.5 Impedance and phase angle change due to the biofilm form on the surface of uncoated SS electrodes.

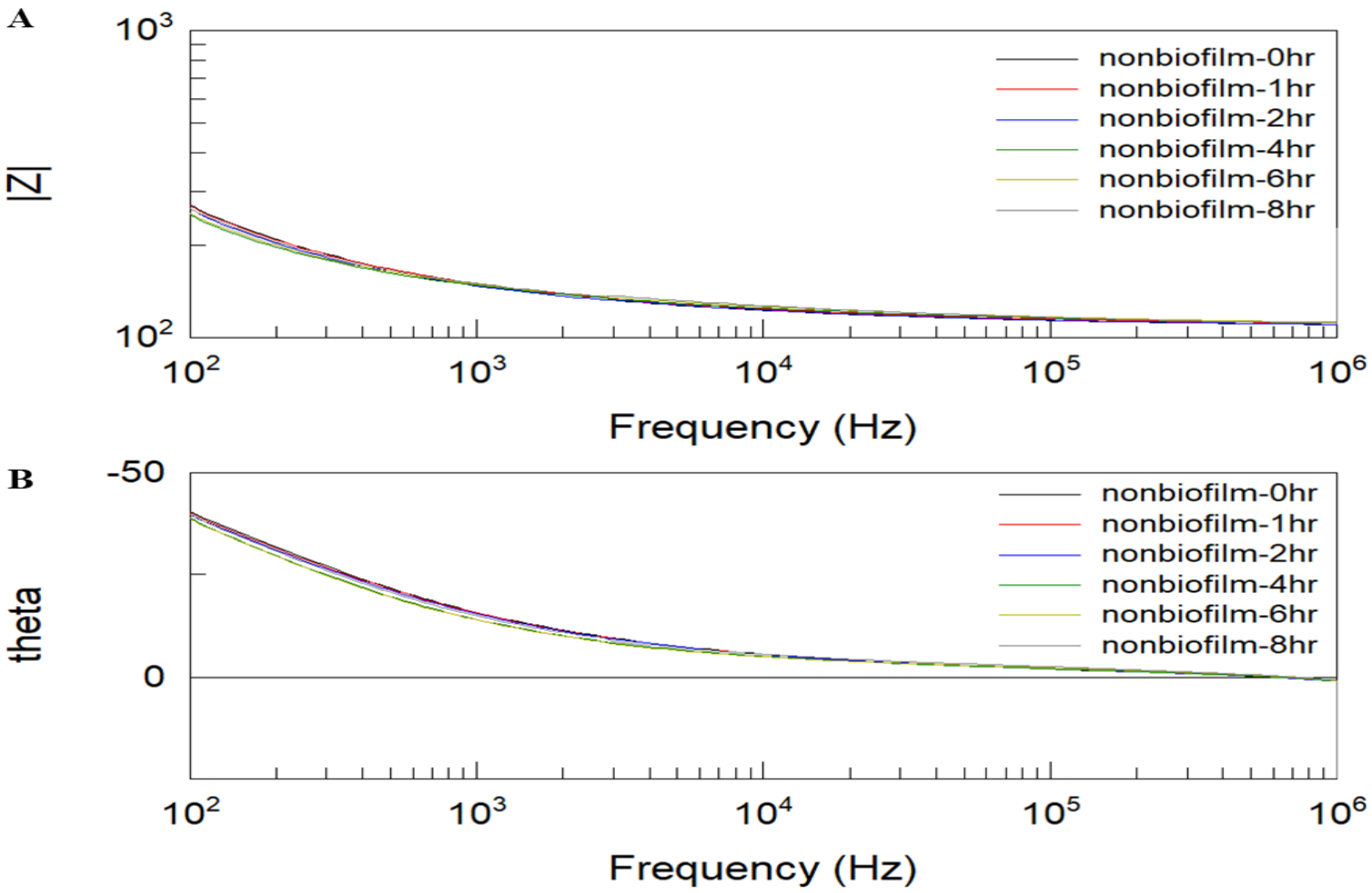

Figure 5.6 Impedance and phase angle slightly change due to the non-biofilm bacterial cell attached to the surface of uncoated SS electrodes.

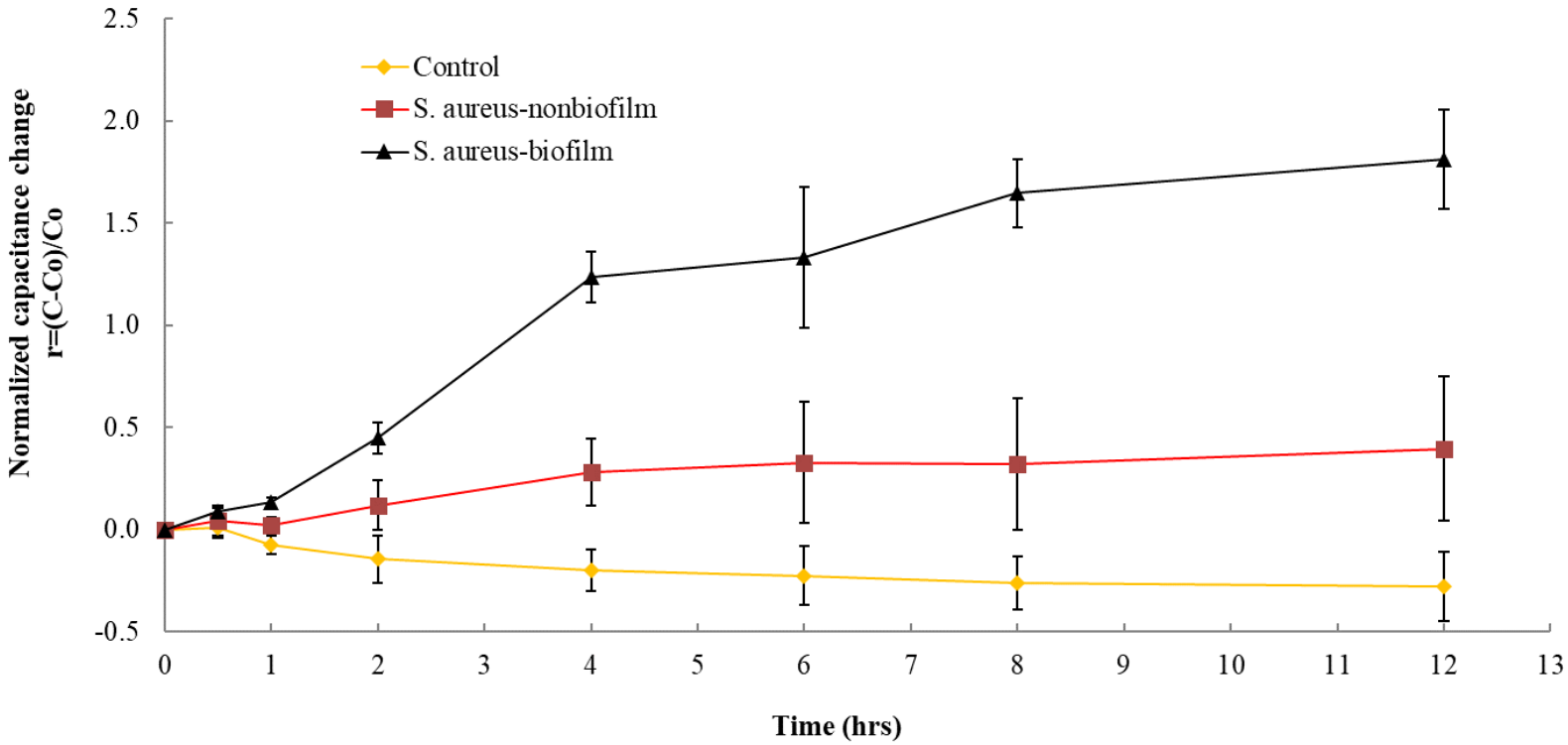

Figure 5.7 Interfacial capacitance change due to the bacteria growth in the EIS adapted wells.

5.3.3 Impedance with an anti-biofilm TMS coating layer

Comparing the biofilm formation on the TMS coated to coated SS electrodes, we found that the interfacial capacitance only has a small increase. The planktonic bacterial cells have difficulty attaching to the TMS coated layer to develop biofilm matrixes on the electrode's surface [97, 99].

The small increase of the capacitance could be due to the few bacterial cells attaches t to the surface and develop to biofilm. Previously researchers[96, 100] have studied TMS coated layer inhibit *S. epidermidis* and *S. aureus* biofilm formation on the surface of SS sheet and silicone surfaces. Their SEM and confocal laser scanning microscope images showed that one few biofilm matrices grew on the coated layer. Our EIS measurements are in agreement with their finding by imaging studies.

5.4. Conclusion

We have described a new method to study biofilm on the implant materials. Based on the data, it appears that the interfacial capacitance increases during bacterial cell attachments, biofilm formation, and biofilm growth on the electrodes' surface in a manner that is proportional to the load of the bacterial cells present. We have also used this EIS based biosensor/bioassay to study the effectiveness of anti-biofilm coating material on the implant material.

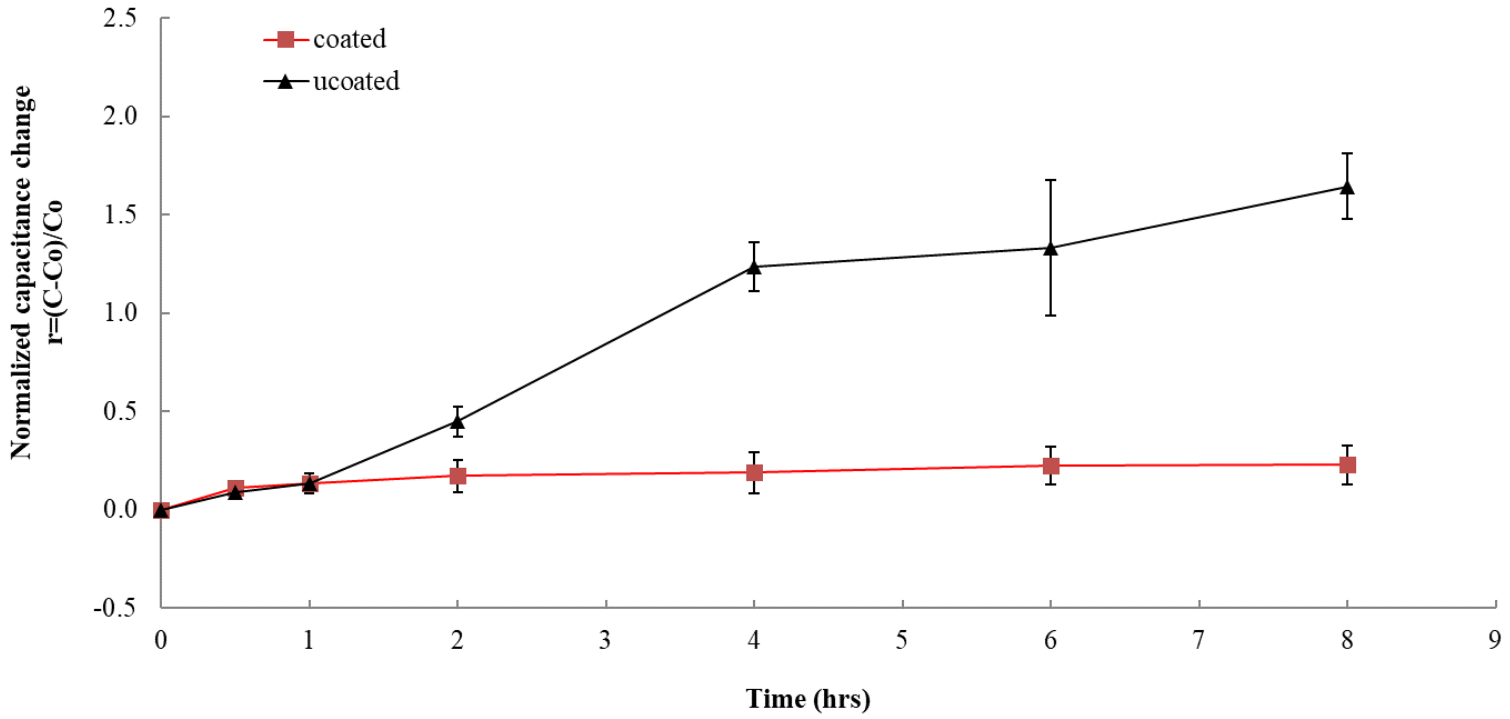

Figure 5.8 Interfacial capacitance only has a small increase on the TMS coated SS electrodes

5.5 Future research

The fact that our method is electrical and lends itself to easy parallelization, potentially enables researchers do perform high-throughput screens for materials that prevent the formation of biofilms on surfaces and/or for methods/chemicals that eliminate biofilms after they are formed.

Also, since we believe that the increase in the interfacial capacitance is proportional to a load of cells (CFUs) present in the biofilm, we believe that if these cells are killed, we should be able to observe the corresponding decrease as well. Hence, this method also has the potential to as a bioassay for cell culture studies, such as cell toxicity for cells that are typically grown on surfaces. Researchers have reported that cells' gap size on an electrode[103], cell coverage on an electrode[103], cell growth, cell death, and cell movement can contribute to the impedance change. We believe that focusing on interfacial capacitance change can provide more accurate information for these studies.

It may also be possible for this biosensor to be built-in within implanted surfaces such as orthopedic implants and provide an early warning system for the biofilm formation there. Once fully formed on implanted surfaces, it is almost impossible to eliminate these biofilms, and a multiple new surgeries often need to be done to take out the implant, treat the infected region with antibiotics, allow time for the region to heal, and put in a fresh implant. An early warning system will enable treatment with oral antibiotics and prevent huge amounts of trauma to the affected patients, while also saving huge cost to the healthcare system.

APPENDIX

TB detection

Table A1-1 Statistical analysis of m-EIS measurement. The Mann-Whitney U values less than or equal to the critical value (in this case, critical value = 2) indicates a significant difference between the bulk capacitance values at that time interval with respect to the baseline. (S = significant difference, NS = not significant difference)

Control 1 (No bacteria)			Control 2 (No Mtb)			50 CFU/ml (Mtb)			500 CFU/ml (Mtb)		
time (hr)	U value	Comparison with baseline	time (hr)	U value	Comparison with baseline	time (hr)	U value	Comparison with baseline	time (hr)	U value	Comparison with baseline
0	-	-	0	-	-	0	-	-	0	-	-
0.5	7	NS	0.5	7	NS	0.5	12	NS	0.5	1	S
1	10	NS	1	10	NS	1	3.5	NS	1	1	S
1.5	5	NS	1.5	5	NS	1.5	10	NS	1.5	0	S
2	7.5	NS	2	7.5	NS	2	9	NS	2	0	S
2.5	3	NS	2.5	3	NS	2.5	11	NS	2.5	0	S
3	12	NS	3	12	NS	3	6	NS	3	0	S

5,000 CFU/ml (Mtb)			50,000 CFU/ml (Mtb)			500,000 CFU/ml (Mtb)		
time (hr)	U value	Comparison with baseline	time (hr)	U value	Comparison with baseline	time (hr)	U value	Comparison with baseline
0	-	-	0	-	-	0	-	-
0.5	0	S	0.5	0	S	0.5	4	NS
1	0	S	1	0	S	1	0	S
1.5	0	S	1.5	0	S	1.5	0	S
2	0	S	2	0	S	2	0	S
2.5	0	S	2.5	0	S	2.5	0	S
3	0	S	3	0	S	3	0	S

LAB detection

Table A2-1 filtration results for *L. acidophilius* and yeast

Before		After (Yeast)					After (*L. acidophilius*)				
Yeast	L. acidophilius	trail 1	trail 2	trail 3	avrage	std	trail 1	trail 2	trail 3	avrage	std
8.8E+08	2.5E+07	0.0E+00	0.0E+00	0.0E+00	0.0E+00	0.0E+00	5.6E+05	6.4E+05	5.1E+05	5.7E+05	6.6E+04
8.8E+08	2.5E+05	0.0E+00	0.0E+00	0.0E+00	0.0E+00	0.0E+00	2.8E+04	2.2E+04	2.5E+04	2.5E+04	3.0E+03
8.8E+08	2.5E+03	0.0E+00	0.0E+00	0.0E+00	0.0E+00	0.0E+00	3.3E+02	2.9E+02	3.1E+02	3.1E+02	2.0E+01

Table A2-2 filtration results for *L. fermentum* and yeast

Before		After (Yeast)					After (*L. fermentum*)				
Yeast	L. fermentum	trail 1	trail 2	trail 3	avrage	std	trail 1	trail 2	trail 3	avrage	std
8.8E+08	2.2E+07	0.0E+00	0.0E+00	0.0E+00	0.0E+00	0.0E+00	1.3E+06	1.1E+06	1.0E+06	1.1E+06	1.5E+05
8.8E+08	2.2E+05	0.0E+00	0.0E+00	0.0E+00	0.0E+00	0.0E+00	1.5E+04	2.0E+04	2.1E+04	1.9E+04	3.2E+03
8.8E+08	2.2E+03	0.0E+00	0.0E+00	0.0E+00	0.0E+00	0.0E+00	3.8E+02	4.7E+02	4.2E+02	4.2E+02	4.3E+01

Table A2-3 filtration results for *L. Casei* and yeast

Before		After (Yeast)					After (*L. Casei*)				
Yeast	L. acidophilius	trail 1	trail 2	trail 3	avrage	std	trail 1	trail 2	trail 3	avrage	std
8.8E+08	1.5E+07	0.0E+00	0.0E+00	0.0E+00	0.0E+00	0.0E+00	1.1E+06	9.5E+05	1.0E+06	1.0E+06	7.6E+04
8.8E+08	1.5E+05	0.0E+00	0.0E+00	0.0E+00	0.0E+00	0.0E+00	5.0E+03	5.5E+03	9.0E+03	6.5E+03	2.2E+03
8.8E+08	1.5E+03	0.0E+00	0.0E+00	0.0E+00	0.0E+00	0.0E+00	5.0E+02	6.0E+02	5.8E+02	5.6E+02	5.3E+01

Biofilm detection

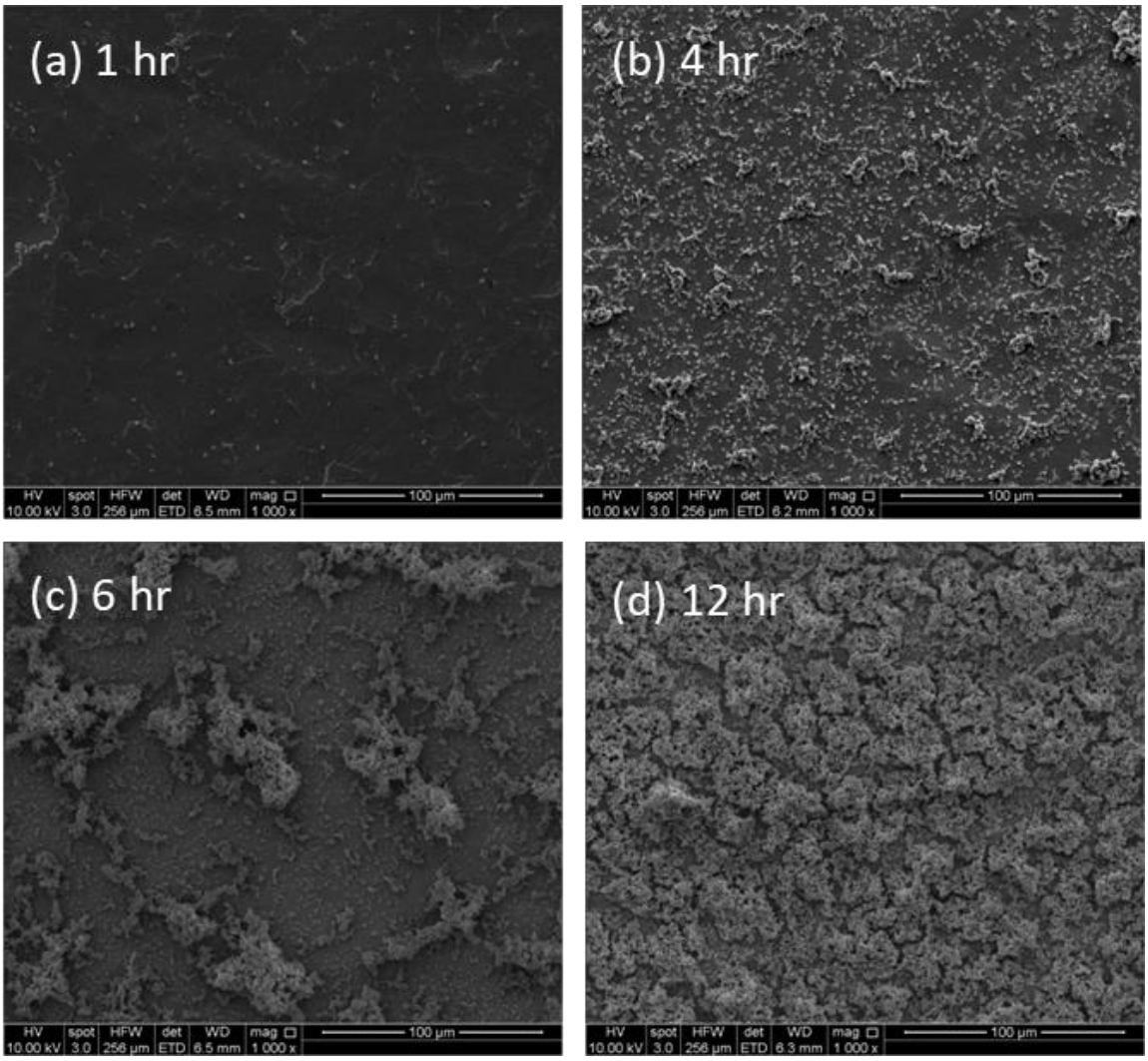

Figure A3-1, Scanning electron microscopy (SEM) of biofilm on uncoated SS sheets.

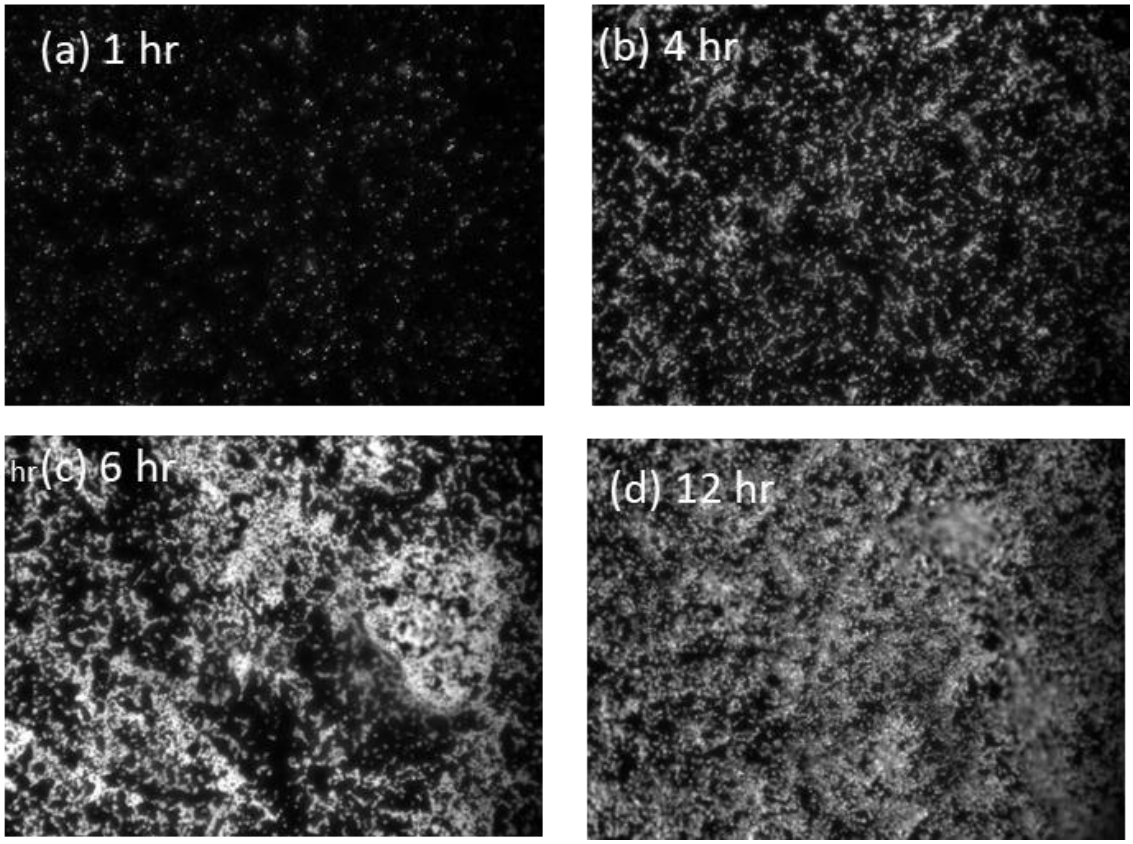

Figure A3-2 Fluorescence image of biofilm on uncoated SS sheets

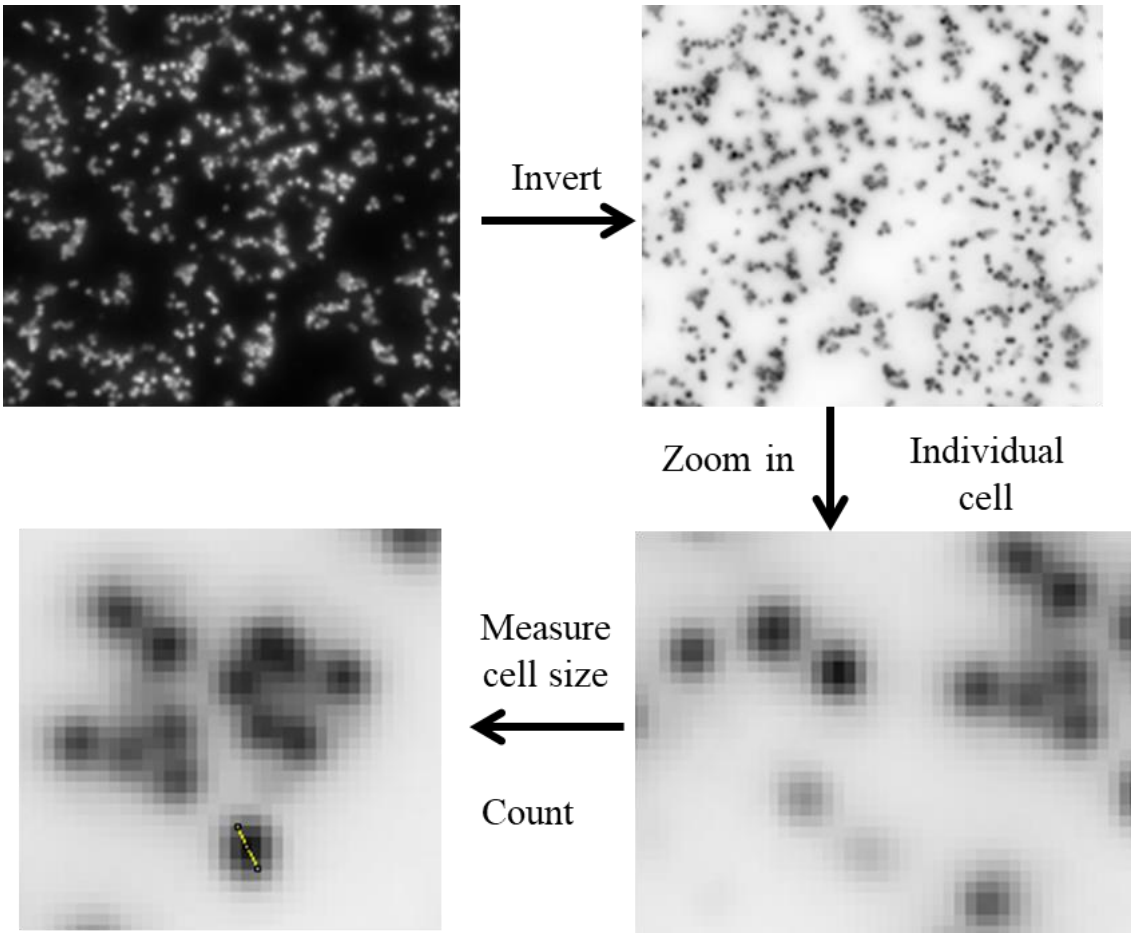

Figure A3-3 Quantitatively analyze the cell number on the electrode. Cell number per square pixel is counted by ITCN: Image-based Tool for Counting Nuclei http://rsb.info.nih.gov/ij/plugins/itcn.html

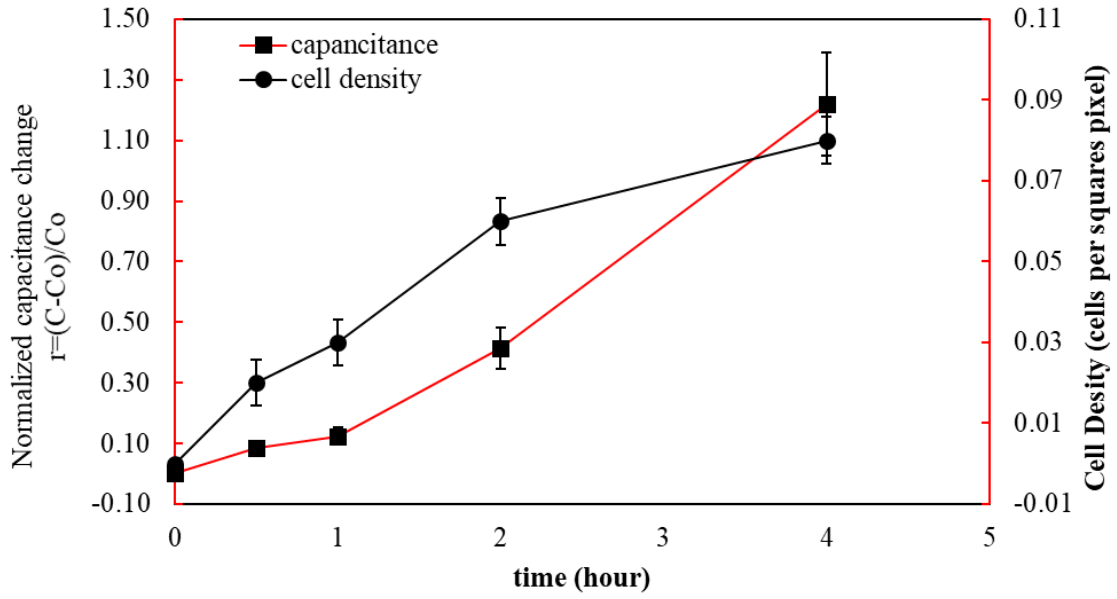

Figure A3-4 Correlation between the interfacial capacitance change and the cell density on the electrode's surface

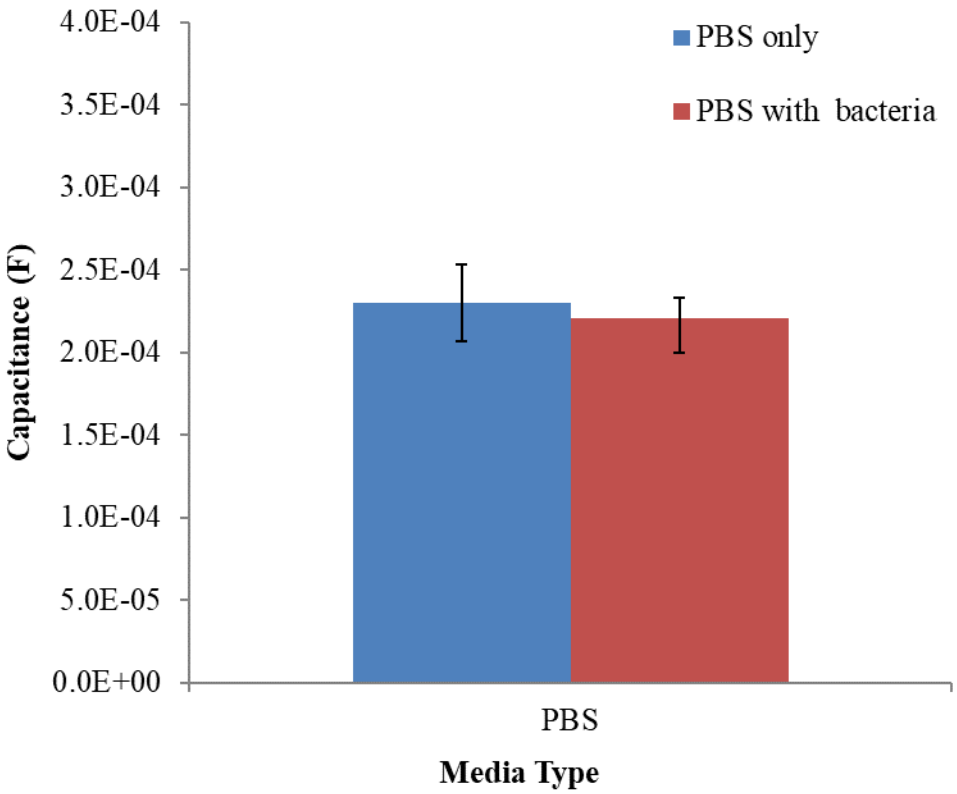

Figure A3-5 Investigate the interfacial capacitance change due to the planktonic bacteria deposited on the electrode surface.

Study the interfacial capacitance change due to the planktonic bacteria deposited on the electrode surface

1) Incubate bacteria to ~10^9 CFU/ml in THY media
2) Centrifuge at 2000 rpm for 10 minutes and remove THY media
3) Resuspend bacteria cells in 1x PBS solution
4) Inject 1 ml of bacterial suspension in 1x PBS solution into EIS adapted well.
5) Perform the EIS test for 1x PBS solution and bacterial cell suspension in 1x PBS solution, respectively.
6) Comparing the interfacial capacitance due to the bacterial cell in the testing solution

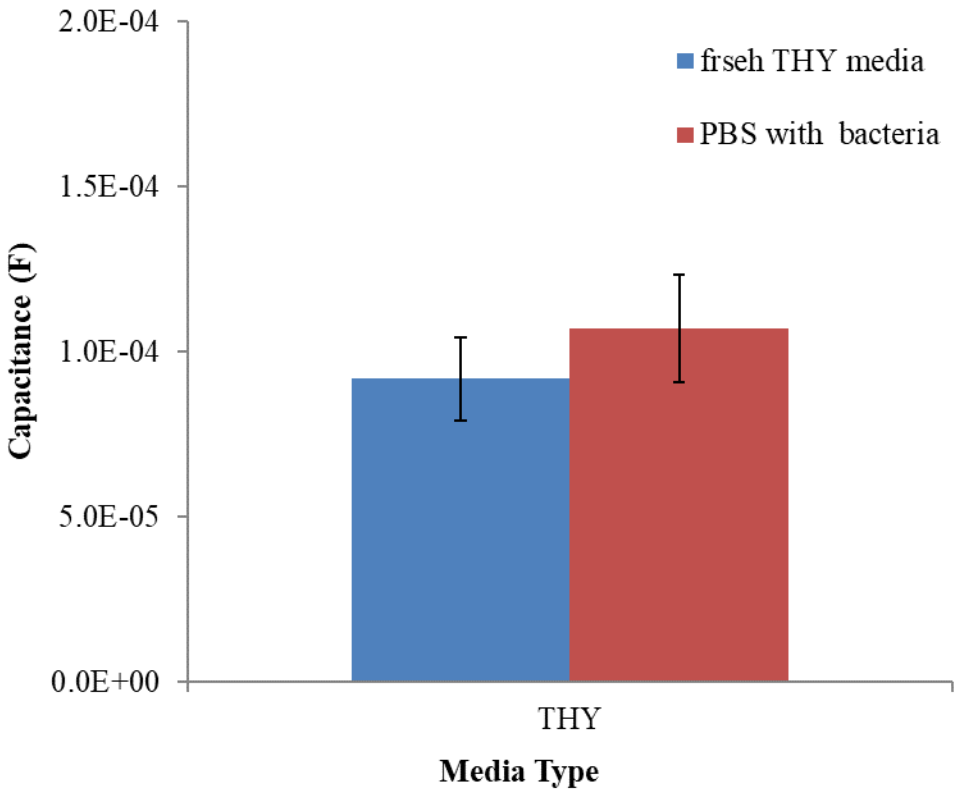

Figure A3-6 Investigate the interfacial capacitance change due to the bacteria metabolism

Study the interfacial capacitance change due to the bacteria metabolism (aged media)

1) Incubate bacteria to ~10^9 CFU/ml in THY media.
2) Centrifuge at 2000 rpm for 10 minutes and collect the aged THY media.
3) Inject 1 ml of aged THY media into EIS adapted well.
4) Perform the EIS test for fresh THY media and the aged, respectively. Comparing the interfacial capacitance due to bacteria metabolism.

LIST OF REFERENCES

1. Lane, N., *The unseen world: reflections on Leeuwenhoek (1677) 'Concerning little animals'.* Philosophical transactions of the Royal Society of London. Series B, Biological sciences, 2015. **370**(1666): p. 20140344.
2. Kollef, M.H., et al., *Inadequate antimicrobial treatment of infections: a risk factor for hospital mortality among critically ill patients.* Chest, 1999. **115**(2): p. 462-474.
3. Sengupta, S., D.A. Battigelli, and H.-C. Chang, *A micro-scale multi-frequency reactance measurement technique to detect bacterial growth at low bio-particle concentrations.* Lab on a Chip, 2006. **6**(5): p. 682-692.
4. Smith, J.M., et al., *A new method for the detection of microorganisms in blood cultures: Part I. Theoretical analysis and simulation of blood culture processes.* The Canadian journal of chemical engineering, 2008. **86**(5): p. 947-959.
5. Sengupta, S., S. Puttaswamy, and H.-C. Chang, *Rapid Detection of Viable Bacteria System and Method*. 2014: USA.
6. Asami, K., *Characterization of Biological Cells by Dielectric Spectroscopy.* Journal of Non-Crystalline Solids, 2002. **305**: p. 268-277.
7. Poortinga, A.T., R. Bos, and H.J. Busscher, *Measurement of charge transfer during bacterial adhesion to an indium tin oxide surface in a parallel plate flow chamber* Journal of Microbiological Methods, 1999. **38**(3): p. 183-189.
8. Swaminathan, B. and P. Feng, *Rapid detection of food-borne pathogenic bacteria.* Annual review of microbiology, 1994. **48**(1): p. 401-426.

9. Richards, J., et al., *Electronic measurement of bacterial growth.* Journal of physics E: Scientific instruments, 1978. **11**(6): p. 560.

10. Yang, L. and R. Bashir, *Electrical/electrochemical impedance for rapid detection of foodborne pathogenic bacteria.* Biotechnology advances, 2008. **26**(2): p. 135-150.

11. Richards, J.C.S., et al., *Electronic measurement of bacterial growth.* Journal of Physics E: Scientific Instruments, 1978. **11**: p. 560-568.

12. Cady, P., *Rapid automated bacterial identification by impedance measurement*, in *New Approaches to the Identijication of Microorganisms*, C.G. Heden and T. Illeni, Editors. 1975. p. 74-99.

13. Firstenberg-Eden, R. and J. Zindulis, *Electrochemical changes in media due to microbial metabolism.* Journal of Microbiological Methods, 1984. **2**(2): p. 103-115.

14. Wawerla, M., et al., *Impedance Microbiology: Applications in Food Hygiene.* Journal of Food Protection, 1999. **62**(12): p. 1488-1469.

15. Yang, L., C. Ruan, and Y. Li, *Detection of viable Salmonella typhimurium by impedance measurement of electrode capacitance and medium resistance* Biosensors and Bioelectronics, 2003. **19**(5): p. 495-502.

16. Yang, L., et al., *Conductivity and pH dual detection of growth profile of healthy and stressed Listeria monocytogenes.* Biotechnology and Bioengineering, 2005. **92**(6): p. 685-694.

17. Sengupta, S., D.A. Battigelli, and H.-C. Chang, *A micro-scale multi-frequency reactance measurement technique to detect bacterial growth at low bio-particle concentrations.* Lab on a Chip, 2006. **6**: p. 682-692.

18. Felice, C.J. and M.E. Valentinuzzi, *Medium and interface components in impedance microbiology.* IEEE Transactions on Biomedical Engineering, 1999. **46**(12): p. 1483-1487.

19. Puttaswamy, S. and S. Sengupta, *Rapid detection of bacterial proliferation in food samples using microchannel impedance measurements at multiple frequencies.* Sensing and Instrumentation for Food Quality and Safety, 2010. **4**(3): p. 108-118.

20. Puttaswamy, S. and S. Sengupta. *Rapid Detection of Bacteria in Blood for the Early Diagnosis of Sepsis*. in *Annual Meeting of the American Institute of Chemical Engineers*. 2010. Salt Lake City, UT.

21. Puttaswamy, S., B.D. Lee, and S. Sengupta, *Novel Electrical Method for Early Detection of Viable Bacteria in Blood Cultures.* Journal of Clinical Microbiology, 2011. **49**(6): p. 2286-2289.

22. Høiby, N., et al., *Antibiotic resistance of bacterial biofilms.* International journal of antimicrobial agents, 2010. **35**(4): p. 322-332.

23. Rasamiravaka, T., et al., *The formation of biofilms by Pseudomonas aeruginosa: a review of the natural and synthetic compounds interfering with control mechanisms.* BioMed research international, 2015. **2015**.

24. Stubbe, M. and J. Gimsa, *Maxwell's mixing equation revisited: characteristic impedance equations for ellipsoidal cells.* Biophysical journal, 2015. **109**(2): p. 194-208.

25. McClendon, J., *COLLOIDAL PROPERTIES OF THE SURFACE OF THE LIVING CELL II. ELECTRIC CONDUCTIVITY AND CAPACITY OF BLOOD TO ALTERNATING CURRENTS OF LONG DURATION AND VARYING IN FREQUENCY FROM 260 TO 2,000,000 CYCLES PER SECOND.* Journal of Biological Chemistry, 1926. **69**(2): p. 733-754.

26. Hanai, T., D.A. Haydon, and J. Taylor, *An investigation by electrical methods of lecithin-in-hydrocarbon films in aqueous solutions.* Proceedings of the Royal Society of London. Series A. Mathematical and Physical Sciences, 1964. **281**(1386): p. 377-391.

27. Coster, H.G., T.C. Chilcott, and A.C. Coster, *Impedance spectroscopy of interfaces, membranes and ultrastructures.* Bioelectrochemistry and Bioenergetics, 1996. **40**(2): p. 79-98.

28. Fricke, H., *The electric conductivity and capacity of disperse systems.* Physics, 1931. **1**(2): p. 106-115.

29. Foster, K.R., J.M. Bidinger, and D. Carpenter, *The electrical resistivity of cytoplasm.* Biophysical journal, 1976. **16**(9): p. 991-1001.

30. Grahame, D.C., *The electrical double layer and the theory of electrocapillarity.* Chemical reviews, 1947. **41**(3): p. 441-501.

31. Wang, H. and L. Pilon, *Accurate simulations of electric double layer capacitance of ultramicroelectrodes.* The Journal of Physical Chemistry C, 2011. **115**(33): p. 16711-16719.

32. Masliyah, J.H. and S. Bhattacharjee, *Electrokinetic and colloid transport phenomena*. 2006: John Wiley & Sons.

33. DeRosa, J.F. and R.B. Beard, *Linear AC electrode polarization impedance at smooth noble metal interfaces.* IEEE Transactions on Biomedical Engineering, 1977(3): p. 260-268.

34. Giaever, I. and C.R. Keese, *Use of electric fields to monitor the dynamical aspect of cell behavior in tissue culture.* IEEE Transactions on Biomedical Engineering, 1986(2): p. 242-247.

35. Keese, C.R. and I. Giaever, *A biosensor that monitors cell morphology with electrical fields.* IEEE Engineering in Medicine and Biology Magazine, 1994. **13**(3): p. 402-408.

36. Seriburi, P., et al. *Using Electric Cell-Substrate Impedance Sensing to Measure Changes in the Projected Area of Individual Cells*. in *TRANSDUCERS 2007-2007 International Solid-State Sensors, Actuators and Microsystems Conference*. 2007. IEEE.

37. Olmo, A. and A. Yúfera. *Finite element simulation of microelectrodes for bio-impedance sensor applications*. in *2010 First International Conference on Sensor Device Technologies and Applications*. 2010. IEEE.

38. WHO, *Tuberculosis.*

39. Esposito, S., et al., *Efficacy, safety, and tolerability of a 24-month treatment regimen including delamanid in a child with extensively drug-resistant tuberculosis: A case report and review of the literature.* Medicine, 2016. **95**(46): p. e5347-e5347.
40. CDC, *TB Treatment for Children.*
41. WHO, *CHEST RADIOGRAPHY IN TUBERCULOSIS DETECTION*
42. Lu, C., et al., *A systematic review of reported cost for smear and culture tests during multidrug-resistant tuberculosis treatment.* PloS one, 2013. **8**(2): p. e56074.
43. WHO, *Guidelines for the programmatic management of drug-resistant tuberculosis, 2018 update.*
44. Chakravorty, S., et al., *The New Xpert MTB/RIF Ultra: Improving Detection of Mycobacterium tuberculosis and Resistance to Rifampin in an Assay Suitable for Point-of-Care Testing.* mBio, 2017. **8**(4): p. e00812-17.
45. Friedrich, S.O., et al., *Assessment of the sensitivity and specificity of Xpert MTB/RIF assay as an early sputum biomarker of response to tuberculosis treatment.* The lancet Respiratory medicine, 2013. **1**(6): p. 462-470.
46. Nicol, M.P., *Xpert MTB/RIF: monitoring response to tuberculosis treatment.* The lancet Respiratory medicine, 2013. **1**(6): p. 427-428.
47. Banada, P.P., et al., *Containment of bioaerosol infection risk by the Xpert MTB/RIF assay and its applicability to point-of-care settings.* Journal of clinical microbiology, 2010. **48**(10): p. 3551-3557.

48. Sharma, B., et al., *Evaluation of a rapid differentiation test for Mycobacterium tuberculosis from other mycobacteria by selective inhibition with p-nitrobenzoic acid using MGIT 960.* Journal of laboratory physicians, 2010. **2**(2): p. 89.

49. Puttaswamy, S., et al., *Multi-frequency Microchannel Electrical Impedance (m-EIS) Method for the Rapid Detection of Proliferating Microorganisms, and their Rapid Quantification.* Journal of Pure and Applied Microbiology, 2017. **11**(3): p. 1219-1237.

50. Kargupta, R., et al., *Rapid culture-based detection of living mycobacteria using microchannel electrical impedance spectroscopy (m-EIS).* Biological Research, 2017. **50**(1): p. 21.

51. Kargupta, R., et al., *Detection by death: A rapid way to detect viable slow-growing microorganisms achieved using microchannel Electrical Impedance Spectroscopy (m-EIS).* Technology, 2018. **6**(01): p. 24-35.

52. Nakedi, K.C., et al., *Comparative Ser/Thr/Tyr phosphoproteomics between two mycobacterial species: the fast growing Mycobacterium smegmatis and the slow growing Mycobacterium bovis BCG.* Frontiers in microbiology, 2015. **6**: p. 237.

53. Moriwaki, Y., et al., *Mycobacterium bovis Bacillus Calmette-Guerin and its cell wall complex induce a novel lysosomal membrane protein, SIMPLE, that bridges the missing link between lipopolysaccharide and p53-inducible gene, LITAF (PIG7), and estrogen-inducible gene, EET-1.* Journal of Biological Chemistry, 2001. **276**(25): p. 23065-23076.

54. Yamada, H., et al., *Preparation of mycobacteria-containing artificial sputum for TB panel testing and microscopy of sputum smears.* The International Journal of Tuberculosis and Lung Disease, 2006. **10**(8): p. 899-905.

55. Butler, T.E., et al., *Direct-from-sputum rapid phenotypic drug susceptibility test for mycobacteria.* PloS one, 2020. **15**(8): p. e0238298.

56. Puttaswamy, S. and S. Sengupta, *Rapid detection of bacterial proliferation in food samples using microchannel impedance measurements at multiple frequencies.* Sensing and Instrumentation for Food Quality and Safety, 2010. **4**(3-4): p. 108-118.

57. Puttaswamy, S., B.D. Lee, and S. Sengupta, *Novel electrical method for early detection of viable bacteria in blood cultures.* Journal of clinical microbiology, 2011.

58. Peres-Brexó, R. and A.S. Sant'Ana, *Impact and significance of microbial contamination during fermentation for bioethanol production. .* Renewable and Sustainable Energy Reviews, 2017. **73**: p. 423-434.

59. Association, R.F., *Annual U.S. Fuel Ethanol Production.* 2019.

60. Rich, J.O., et al., *Resolving bacterial contamination of fuel ethanol fermentations with beneficial bacteria – An alternative to antibiotic treatment. .* Bioresource Technology, 2018. **427**(357-362).

61. Skinner, K.A. and T.D. Leathers, *Bacterial contaminants of fuel ethanol production.* Journal of Industrial Microbiology and Biotechnology, 2004. **31**(9): p. 410-408.

62. Rich, J.O., et al., *Biofilm formation and ethanol inhibition by bacterial contaminants of biofuel fermentation.* Bioresource Technology, 2015. **196**: p. 347-354.

63. Narendranath, N.V., et al., *Effects of lactobacilli on yeast-catalyzed ethanol fermentations.* Applied and Environmental Microbiology, 1997. **63**: p. 4158-4163.

64. Hynes, S., et al., *Use of virginiamycin to control the growth of lactic acid bacteria during alcohol fermentation.* Journal of Industrial Microbiology and Biotechnology, 1997. **18**(4): p. 284-291.

65. Narendranath, N., et al., *Effects of lactobacilli on yeast-catalyzed ethanol fermentations.* Applied and Environmental Microbiology, 1997. **63**(11): p. 4158-4163.

66. Muthaiyan, A., A. Limayem, and S. Ricke, *Antimicrobial strategies for limiting bacterial contaminants in fuel bioethanol fermentations.* Progress in Energy and Combustion Science, 2011. **37**(3): p. 351-370.

67. Bischoff, K.M., et al., *Modeling Bacterial Contamination of Fuel Ethanol Fermentation.* Biotechnology and Bioengineering, 2009. **103**: p. 117-122.

68. Brexo, R.P. and A.S. Sant'Ana, *Impact and significance of microbial contamination during fermentation for bioethanol production.* Renewable and Sustainable Energy Reviews, 2017. **72**: p. 423-434.

69. Beckner, M., M.L. Ivey, and T.G. Phister, *Microbial contamination of fuel ethanol fermentations.* Letters in Applied Microbiology, 2011.

70. Young, J., P.J. Lee, and A. Di Gioia, *Fast HPLC analysis for fermentation ethanol processes.* Waters Corporation, Milford, MA, 2006.

71. EGERV RN, M., et al., *Antibiotic susceptibility profiles of Lactobacillus reuteri and Lactobacillus fermentum.* Journal of food protection, 2007. **70**(2): p. 412-418.

72. Nobile, J., *Use of membrane filter technique in the microbiological control for the brewing industry.* Appl. Environ. Microbiol., 1967. **15**(4): p. 736-737.

73. Foley, G., *A review of factors affecting filter cake properties in dead-end microfiltration of microbial suspensions.* Journal of Membrane Science, 2006. **274**(1-2): p. 38-46.

74. Zhang, D., et al., *Magnetic nanoparticle-mediated isolation of functional bacteria in a complex microbial community.* The ISME journal, 2015. **9**(3): p. 603-614.

75. Shan, Z., et al., *Bacteria capture, lysate clearance, and plasmid DNA extraction using pH-sensitive multifunctional magnetic nanoparticles.* Analytical biochemistry, 2010. **398**(1): p. 120-122.

76. Lin, Y.-S., et al., *Affinity capture using vancomycin-bound magnetic nanoparticles for the MALDI-MS analysis of bacteria.* Analytical chemistry, 2005. **77**(6): p. 1753-1760.

77. Beckner, M., M.L. Ivey, and T.G. Phister, *Microbial contamination of fuel ethanol fermentations.* Letters in applied microbiology, 2011. **53**(4): p. 387-394.

78. Basílio, A., et al., *Detection and identification of wild yeast contaminants of the industrial fuel ethanol fermentation process.* Current Microbiology, 2008. **56**(4): p. 322-326.

79. de Souza Liberal, A., et al., *Identification of Dekkera bruxellensis as a major contaminant yeast in continuous fuel ethanol fermentation.* Journal of Applied Microbiology, 2007. **102**(2): p. 538-547.

80. Mah, T.-F.C. and G.A. O'toole, *Mechanisms of biofilm resistance to antimicrobial agents.* Trends in microbiology, 2001. **9**(1): p. 34-39.

81. Stewart, P.S., *Mechanisms of antibiotic resistance in bacterial biofilms.* International journal of medical microbiology, 2002. **292**(2): p. 107.

82. González, J.F., M.M. Hahn, and J.S. Gunn, *Chronic biofilm-based infections: skewing of the immune response.* Pathogens and Disease, 2018. **76**(3).

83. Costerton, J., L. Montanaro, and C.R. Arciola, *Biofilm in implant infections: its production and regulation.* The International journal of artificial organs, 2005. **28**(11): p. 1062-1068.

84. Busscher, H., et al., *Biofilm formation on dental restorative and implant materials.* Journal of dental research, 2010. **89**(7): p. 657-665.

85. Mack, D., et al., *Biofilm formation in medical device-related infection.* The International journal of artificial organs, 2006. **29**(4): p. 343-359.

86. Wolcott, R. and S. Dowd, *The role of biofilms: are we hitting the right target?* Plastic and reconstructive surgery, 2011. **127**: p. 28S-35S.

87. Ribeiro, S.M., et al., *New frontiers for anti-biofilm drug development.* Pharmacology & Therapeutics, 2016. **160**: p. 133-144.

88. Singha, P., J. Locklin, and H. Handa, *A review of the recent advances in antimicrobial coatings for urinary catheters.* Acta biomaterialia, 2017. **50**: p. 20-40.

89. Ivanova, A., et al., *Layer-by-layer decorated nanoparticles with tunable antibacterial and antibiofilm properties against both gram-positive and gram-negative bacteria.* ACS applied materials & interfaces, 2018. **10**(4): p. 3314-3323.

90. Donlan, R.M., *Biofilms: microbial life on surfaces.* Emerging infectious diseases, 2002. **8**(9): p. 881.

91. Ma, Y., et al., *Inhibition of Staphylococcus epidermidis biofilm by trimethylsilane plasma coating.* Antimicrobial agents and chemotherapy, 2012: p. AAC. 01739-12.

92. Ramasamy, R.P., et al., *Impact of initial biofilm growth on the anode impedance of microbial fuel cells.* Biotechnology and bioengineering, 2008. **101**(1): p. 101-108.

93. Silley, P. and S. Forsythe, *Impedance microbiology—a rapid change for microbiologists.* Journal of Applied Bacteriology, 1996. **80**(3): p. 233-243.

94. Paredes, J., et al., *Real time monitoring of the impedance characteristics of Staphylococcal bacterial biofilm cultures with a modified CDC reactor system.* Biosensors and Bioelectronics, 2012. **38**(1): p. 226-232.

95. Talha, M., C. Behera, and O. Sinha, *A review on nickel-free nitrogen containing austenitic stainless steels for biomedical applications.* Materials Science and Engineering: C, 2013. **33**(7): p. 3563-3575.

96. Chen, M., Q. Yu, and H. Sun, *Novel strategies for the prevention and treatment of biofilm related infections.* International journal of molecular sciences, 2013. **14**(9): p. 18488-18501.

97. Ma, Y., et al., *Inhibition of Staphylococcus epidermidis biofilm by trimethylsilane plasma coating.* Antimicrobial agents and chemotherapy, 2012. **56**(11): p. 5923-5937.

98. Resources, B., *Product Information Sheet for NR-46027.* 2016.

99. Ma, Y., et al., *Novel inhibitors of Staphylococcus aureus virulence gene expression and biofilm formation.* PloS one, 2012. **7**(10): p. e47255.

100. Xu, Y., et al., *Nanoscale plasma coating inhibits formation of Staphylococcus aureus biofilm.* Antimicrobial agents and chemotherapy, 2015. **59**(12): p. 7308-7315.

101. Croes, S., et al., *Staphylococcus aureus biofilm formation at the physiologic glucose concentration depends on the S. aureus lineage.* BMC microbiology, 2009. **9**(1): p. 229.

102. Harris, C.M. and D.B. Kell, *578-THE RADIO-FREQUENCY DIELECTRIC PROPERTIES OF YEAST CELLS MEASURED WITH A RAPID, AUTOMATED, FREQUENCY-DOMAIN DIELECTRIC SPECTROMETER.* Bioelectrochemistry and bioenergetics, 1983. **11**: p. 15-28.

103. Huang, X., et al., *Simulation of microelectrode impedance changes due to cell growth.* IEEE Sensors Journal, 2004. **4**(5): p. 576-583.

104. Stoner, G.E. and S. Srinivasan, *Adsorption of blood proteins on metals using capacitance techniques.* The Journal of Physical Chemistry, 1970. **74**(5): p. 1088-1094.

105. Tuson, H.H. and D.B. Weibel, *Bacteria-surface interactions.* Soft matter, 2013. **9**(18): p. 4368-4380.

VITA

Yongqiang Yang was born in 1979 in China to Guoan Yang and Junying Xia. He enrolled in the Hebei Normal University of Science and Technology, Qinhuangdao, China, in September 2001, and graduated with a Bachelor of Science in Food Science & Processing in July 2005. He also enrolled in the University of Findlay, Ohio in the fall of 2007 and graduated with a Master of Science in Environmental, Health and Safety Management in December 2010. He received his second Master of Science in Environmental Engineering Sciences from the University of Florida in the spring of 2011. He completed his Doctor degree in Biological Engineering in the University of Missouri-Columbia in December 2020.